Det Kgl. Danske Videnskabernes Selskab.
Mathematisk-fysiske Meddelelser. **X**, 4.

MODUS OPERANDI OF THE AIR-JET PULSATOR

BY

JUL. HARTMANN AND BIRGIT TROLLE

WITH 6 PLATES

KØBENHAVN
HOVEDKOMMISSIONÆR: ANDR. FRED. HØST & SØN, KGL. HOF-BOGHANDEL
BIANCO LUNOS BOGTRYKKERI A/S
1930

Introduction.

The air-jet generator for acoustic waves has been described in several papers[1—4]* together with experiments carried out with a view to throwing a light on the general properties of the said generator. The object of the present paper is to record a series of investigations on the modus operandi of the generator. A main member of the same is, as will be known from the papers referred to, an air-jet with a velocity exceeding that of sound. The jet is directed towards the aperture of a cylindrical oscillator or the mouth of a so-called pulsator. There is some reason for believing that the modus operandi is in the main — though possibly not exactly — the same with the two devices. As, however, the period of the oscillations, or pulsations, with the pulsator can be made as long as desired while it is generally exceedingly short with the oscillator, it seemed much easier to study the oscillatory process with the former than with the latter device. The pulsator was therefore chosen as the object of observation in the present investigation.

The pulsation phenomenon, as explained in the papers alluded to above, consists in the pulsator alternately filling with and discharging air when the mouth is adjusted in one of the so-called intervals of instability of the jet. The latter intervals in the main coincide with those parts of

* See List of References pag. 60.

the jet in which the pressure read on a pitot-apparatus increases when the pitot-tube or sound is moved along the axis of the jet in the direction of the latter. As the modus operandi of the generator of course depends on the special properties of the particular air-jet employed, we have found it appropriate, or rather necessary, to review the said properties in the first part of our paper.

I

On an Air-Jet with a Velocity exceeding that of Sound.

1. Production of an Air-Jet with a Velocity exceeding that of Sound.

The main properties of the jet in question have proved to be derivable from the laws of a steady, adiabatic and irrotational flow of a frictionless gas[5,6,7]. From these laws it follows that the characteristics of the flow, that is to say, the pressure p, the density ϱ, the temperature θ, the velocity φ, and the area of the cross-section f of the stream-line tube, are determined solely 1: by one of the said quantities, 2: by the mass of air G transmitted per second through the tube, and 3: by the initial condition i. e. the values p_0, ϱ_0 and θ_0 of p, ϱ and θ corresponding to $\varphi = 0$. For the said laws may be written:

$$(1)\text{—}(3)\quad \frac{\theta}{\theta_0} = \left(\frac{\varrho}{\varrho_0}\right)^{\varkappa-1} = \left(\frac{p}{p_0}\right)^{\frac{\varkappa-1}{\varkappa}} = 1 - \frac{\varkappa-1}{2} \cdot \frac{\varphi^2}{\varkappa R \theta_0}$$

$$(4)\qquad f = \frac{G}{\varrho \varphi}.$$

$\varkappa$ being the ratio $\frac{c_p}{c_v}$ of the specific heats at constant pressure and constant volume and R the constant of Boyle's law.

A discussion of the equations (1)—(4) shows that if the velocity increases in the direction of the flow, then the pressure, the density, and the temperature will decrease in the same direction. The area f of the cross-section of the

stream-line tube will decrease until the velocity has reached a value equal to the velocity of sound characteristic of the state at the corresponding point of the jet. Hereafter f will increase together with the velocity, which now becomes greater than the velocity of sound corresponding to the state at the point considered.

Applying this to a jet of an ideal gas emitted from a container in which the state is given by p_0, ϱ_0, θ_0 and $\varphi = 0$, into the free atmosphere, in which the pressure may be p_e, we may easily see what will be the condition for the production of a jet with a velocity higher than that of sound. The condition is that the jet considered as a bundle of stream-line tubes assumes in one place or other a minimum of cross-section. If it does, the velocity is here determined by

$$\varphi_k^2 = \frac{dp}{d\varrho} = \varkappa R \theta_k \tag{5}$$

where θ_k is the temperature in the said cross-section. Inserting this in (1)—(3), the other characteristics of the jet at the least cross-section are found. They are seen to be determined by

$$\frac{\theta_k}{\theta_0} = \left(\frac{\varrho_k}{\varrho_0}\right)^{\varkappa-1} = \left(\frac{p_k}{p_0}\right)^{\frac{\varkappa-1}{\varkappa}} = \frac{2}{\varkappa+1}. \tag{6)—(7}$$

With atmospheric air $\varkappa = 1.404$ from which $\frac{p_k}{p_0} = 0.527$ or nearly $\frac{1}{1.9}$ while $\frac{\theta_k}{\theta_0} = \frac{1}{1.202}$. From the pressure relation it follows that an air-jet with a velocity higher than that of sound can only be obtained if the critical pressure p_k is higher than the pressure p_e in the atmosphere into which the jet is emitted. Thus with efflux into the free atmosphere the pressure in the container must be higher

than 1.9 atmospheres or the excess-pressure must be greater than 0.9 atmosphere.

It has been found that if the orifice is given the shape of a Laval-Nozzle, fig. 1, the position of the least cross-section of the jet (or of its several stream-line tubes) does not depend on the ratio $\frac{p_0}{p_e}$, while with an obtuse conical bore, fig. 2, the position, which is always close to the least cross-section of the nozzle, depends in some degree on the said ratio[8].

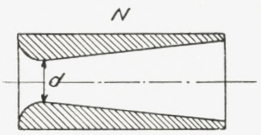

Fig. 1. Laval-Nozzle.

2. Structure of an Air-Jet with a Velocity exceeding that of Sound.

Leaving the nozzle, the jet with the velocity exceeding that of sound will commence by expanding, provided its static pressure is higher than the pressure in the atmosphere into which the jet is emitted. This means that the various particles, in addition to their forward velocity, acquire a radial velocity owing to the difference between the pressure in the jet and the surroundings. The outward motion of the particles will reduce the pressure in the jet, but even after the said pressure has been brought down to the value of the external pressure, the radial motion of the particles will prevail for a while, thereby causing the pressure in the jet to go down below that of the surroundings. The under-pressure in the jet will finally bring the outward motion to an end, and then reverse the direction of the motion so that the particles now move inwards, thereby causing the pressure in the jet to rise again to a value above the external pressure. Now the direction of the motion is again reversed, and the phenomenon described is repeated over and over again. Obviously we must ex-

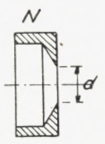

Fig. 2. Obtuse conical Nozzle.

pect the jet to exhibit alternate expansions and contractions of stationary positions with regard to the nozzle.

The structure of a flat jet with a velocity exceeding that of sound discharged through a slit has been investigated theoretically and experimentally by L. Prandtl [9, 10] and his co-workers [11, 12, 13] Prandtl's explanation of the structure is based on the simple laws for a homogeneous flow of air with a velocity exceeding that of sound beyond an edge, in the case in question the edge of the slit through which the jet is discharged. Qualitatively Prandtl's results also apply to the circular jet, the structure of which has been made the subject of several investigations [14, 15, 16]. The structure to be anticipated on the basis of Prandtl's investigation is indicated in fig. 3. The jet is assumed to be discharged from AB, with a velocity just equal to that of sound. It is divided up in sections, the boundaries of which are A_1B_1, A_2B_2, ... The way in which the sections are formed are, according to Prandtl, as follows. From a point A of the edge of the orifice a rarefaction-wave BAB_1 is emitted. In the wave the pressure increases towards the boundary AB of the wave as indicated by the arrow. The wave is reflected from the surface BB_1 of the jet as the wave BA_1B_1. The latter is again reflected from the opposite surface as $B_1A_1B_2$ and so on. Obviously waves like that considered are emitted from all points of the edge of the orifice, thus for instance from B, producing in interaction a structure like that shown in fig. 3. The corresponding distribution

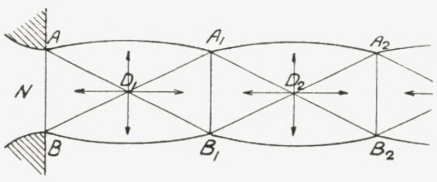

Fig. 3. Structure of Jet with Super Sound-Velocity.

of pressure is indicated by the arrows. The pressure rises from a minimum in the centre D of the jet-section towards the surface of the jet, where it becomes equal to the external pressure, and furthermore towards the boundary lines of the sections A_1B_1, A_2B_2 where the pressure of the orifice or nearly that prevails. In the case considered, the latter pressure is the critical pressure p_k defined in paragraph 1.

A series of photographs of an actual jet are given in fig. 4. Pl. 1. The pictures are produced by means of the method of striæ. They originate from the nozzle *ZI*, see Tab. II, and correspond to the following values of the ratio $\frac{p_0}{p_e}$ of the absolute pressure p_0 in the container and the exterior pressure p_e.

Tab. I.

Fig.	$\frac{p_0}{p_e}$
4 a	2.95
4 b	3.45
4 c	4.02
4 d	4.47
4 e	5.01
4 f	5.43
4 g	5.90
4 h	6.38

The pictures agree fairly well with the diagram fig. 3. The discrepancies will be considered below.

3. The stationary Compression-Wave.

In the present introduction we have still to consider a phenomenon of paramount importance for the modus ope-

randi of the generator in question. The phenomenon is illustrated in fig. 5. The lower part of the picture represents a parallel flow of air which is assumed to extend infinitely in all directions perpendicular to the flow. To the left of the cross-section ab the state of the air is characterized by φ, p, v $\left(v = \frac{1}{\varrho}\right)$. It now turns out that if φ is greater than the velocity of sound, a sudden irreversible change in the state of the flow may take place within an extremely thin layer ab. The pressure and density increase while the velocity and the kinetic energy of the flow decrease. The layer may be identified with a stationary compression-wave of finite amplitude. In German papers it is referred to as a "Verdichtungsstoss". It is well known from several phenomena. Thus the conical wave accompanying a projectile flying with a velocity greater than that of sound, the Mach-wave, is of this description, although the greater part of the said wave is not a perpendicular "Verdichtungsstoss" but an oblique one, fig. 6. In the latter the component of the velocity parallel to the "stoss" passes the same without any change, while in the component perpendicular to the wave a change takes place as in the case shown in fig. 5.

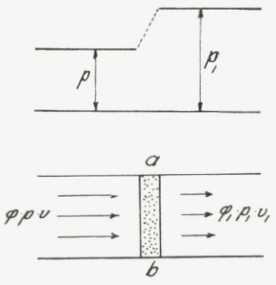

Fig. 5. Perpendicular Compression-Wave.

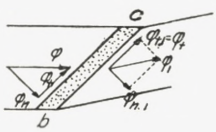

Fig. 6. Oblique Compression-Wave.

While the structure of the compression-wave proper is still to some extent a riddle, it is easy to derive formulae expressing the state behind the compression by that in front of the same[17,18,19]. The theory is based on the suppositions that the cross-section of a stream-line tube is

constant and that no energy or momentum is transmitted to the tube from the adjacent tubes inside the layer of the irreversible process. These assumptions are expressed in the following equations in which the notations of fig. 5 are used

(1) $$\varrho\,\varphi = \varrho_1\,\varphi_1$$

(2) $$\frac{1}{2}\varphi^2 + \frac{\varkappa}{\varkappa - 1} R\theta = \frac{1}{2}\varphi_1^2 + \frac{\varkappa}{\varkappa - 1} R\theta_1$$

(3) $$p + \varrho\,\varphi^2 = p_1 + \varrho_1\,\varphi_1^2 .$$

From (1)—(3) in connection with

(4) $$p = \varrho R\theta \quad \text{and}$$

(5) $$p_1 = \varrho_1 R\theta_1$$

the relations

(6) $$\frac{\varphi_1}{\varphi} = \frac{2}{\varkappa + 1}\left[\frac{\varkappa - 1}{2} + \varkappa\frac{R\theta}{\varphi^2}\right]$$

(7) $$\frac{\varrho_1}{\varrho} = \frac{\varkappa + 1}{2}\left[\frac{\varkappa - 1}{2} + \varkappa\frac{R\theta}{\varphi^2}\right]^{-1}$$

(8) $$\frac{p_1}{p} = \frac{2}{\varkappa + 1}\left[\frac{\varphi^2}{R\theta} - \frac{\varkappa - 1}{2}\right]$$

are derived for the perpendicular compression-wave. As φ is greater than the velocity of sound, that is to say φ^2 greater than $\varkappa R\theta$, it is seen that density and pressure are always raised while the velocity is reduced in the wave. As shown by Prandtl, the velocities φ and φ_1 are connected by the simple formula

(9) $$\varphi\varphi_1 = \varphi_k^2$$

where φ_k is the critical velocity — equal to the velocity of sound at the smallest jet-section — indicated in equation (5) paragraph 1. That is to say

$$\varphi_k^2 = \varkappa R \theta_k = \frac{2\varkappa}{\varkappa + 1} \cdot \frac{p_0}{\varrho_0} \tag{10}$$

p_0 and ϱ_0 being the pressure and density at the outset of the flow where the velocity is zero. As φ is greater than the velocity of sound, it may be concluded from equation (9) that the velocity is reduced by the wave to a value smaller than the velocity of sound.

In case of an oblique compression-wave, fig. 6, (9) is, as shown by Th. Meyer,[11, 19] replaced by

$$\varphi_n \varphi_{n\cdot 1} + \frac{\varkappa - 1}{\varkappa + 1} \varphi_t^2 = \varphi_k^2 \tag{11}$$

while $\varphi_t = \varphi_{t\cdot 1}$.

With a view to illustrating the subject of the present paragraph, attention may again be drawn to the photographs of fig. 4, Pl. 1, in connection with the diagram of fig. 3. It will be noted that the section $D_1 A_1 B_1$, in which the pressure increases and the velocity decreases from D_1 to $A_1 B_1$, gradually becomes a smaller fraction of the whole section $AB A_1 B_1$ when $\frac{p_0}{p_e}$ increases. At the same time each of the boundary lines $D_1 A_1$ and $D_1 B_1$ becomes sharper and undoubtedly develops into an oblique compression-wave. At a value of ab. 3.5 of $\frac{p_0}{p_e}$ the wave is distinct. From ab. $\frac{p_0}{p_e} = 4.8$ the two waves $D_1 A_1$ and $D_1 B_1$ are united by a wave perpendicular to the axis of the jet, that is to say, by a perpendicular compression-wave in which the velocity of the jet is brought down below the velocity of sound. At this stage, therefore, the regular

periodic structure of the jet vanishes because the said structure is dependent on super sound-velocity.

4. Stoppage of an Air-Jet with a Velocity exceeding that of Sound.

The theory of the perpendicular compression-wave in the main accounts for what happens when an air-jet with a velocity greater than that of sound impinges on a wall perpendicular to the jet. In fig. 7, J is the jet discharged from the container C. B is the wall in which we may assume a fine hole to be drilled connecting the front of the wall with a space P beyond, in which the pressure may be measured by means of a manometer. If, as in fig. 7 a, the velocity of the jet is below that of sound, the pressure in the central stream-line tube at the point in which it hits the wall and is stopped by the same should be very nearly that of the container. That is to say, the pressure p'_0, read on the manometer referred to, should be p_0. As a matter of fact it is found to assume that value, showing that the process of efflux and stoppage in this case takes place adiabatically according to the equations (1)—(4) of paragraph 1. Otherwise in the case of fig. 7 b, in which a velocity exceeding that of sound obtains. Here the process of stoppage takes place by two steps. The first step is taken in a compression-

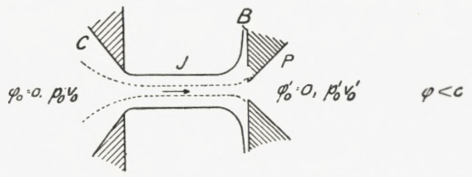

Fig. 7 a. Stoppage of Jet with a Velocity smaller than that of Sound.

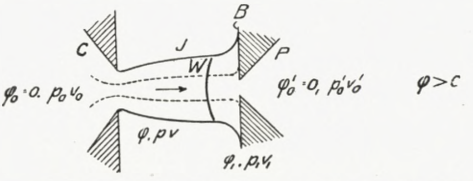

Fig. 7 b. Stoppage of Jet with a Velocity exceeding that of Sound. Compression-Wave W in Front of Wall.

wave W somewhat in front of the wall. Inside the central stream-line tube, W may as a rule be considered as a perpendicular compression-wave, in which the pressure is raised by an irreversible process from the value p just in front of the wave to the value p_1 just beyond the same, while at the same time the kinetic energy of the flow is diminished and the velocity reduced to a value smaller than the velocity of sound. The connection between p_1 and p is expressed by (8) in the preceding paragraph. The second step of the process consists in an adiabatic compression which takes place in the space between W and the wall, and is determined by the equations (1)—(4) of paragraph 1. Applying the said equations and those of the perpendicular compression-wave, an expression for the pressure p'_0 may be derived. With the notations of fig. 7 b we find

$$(1) \qquad p'_0 = 2K\varrho\varphi^2 \cdot \left[\varkappa - \frac{\varkappa-1}{2} \cdot \frac{c^2}{\varphi^2}\right]^{-\frac{1}{\varkappa-1}}$$

where $K = \frac{1}{\varkappa}\left(\frac{\varkappa+1}{2}\right)^{\frac{\varkappa+1}{\varkappa-1}}$ and $c^2 = \varkappa R\theta$.

In (1) the „stoppage-pressure" p'_0 is expressed by the state just in front of the compression-wave. Now, however, the flow from the container down to the front of the compression-wave takes place adiabatically according to the equations (1)—(4) of paragraph 1. This means that the state in front of the wave may be expressed by the characteristics $\varphi_0, p_0, \varrho_0, \theta_0$ of the air in the container in connection with one of the quantities φ, p, ϱ, θ. And so the same must be true for the stoppage-pressure p'_0. Thus for instance p'_0, may be expressed in the following way

$$(2) \qquad \frac{p_0'}{p_0} = \left(\frac{\varkappa+1}{\varkappa-1}\right)^{\frac{\varkappa+1}{\varkappa-1}} \frac{\left(\frac{p_0}{p}\right)^{\frac{\varkappa-1}{\varkappa}} - 1}{\frac{p_0}{p}\left[\frac{4\varkappa}{(\varkappa-1)^2} - \frac{1}{\left(\frac{p_0}{p}\right)^{\frac{\varkappa-1}{\varkappa}} - 1}\right]^{\frac{1}{\varkappa-1}}}.$$

The validity of equation (2) has been put to the test by Stanton[8].

5. The Pitot-Curve.

The air-jet generator for acoustic waves was invented in connection with a study of the structure of the jet by means of a simple pitot-apparatus. Its operational qualities may in a natural way be put in relation to that characteristic of the jet, the pitot-curve, which may be found by means of the said apparatus. With a view to understanding the generator a good deal of work has therefore been done on the study of the pitot-curve.

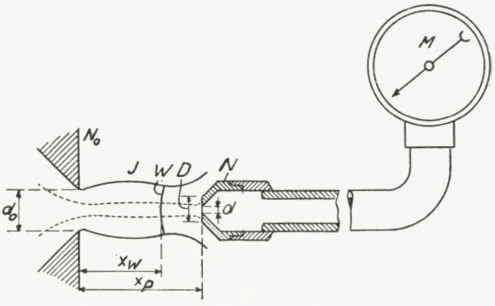

Fig. 8 a. Pitot-Apparatus with Bore.

In fig. 8 a a simple pitot-apparatus is shown. It consists of a nozzle *N* with a fine bore. The nozzle is directed towards the jet *J*. It is connected to a manometer *M*. The apparatus in fig. 8 a is of a special kind. Generally the bore in *N* is replaced by a thin tube, the pitot-sound, fig. 8 b. In a good many cases a steel-tube with an interior diameter of 0.38 mm and a length of about 8 mm has been employed, but curves have also been determined by means of heavier sounds or by nozzles like that in fig. 8 a.

The general aspect of the pitot-curve in the case of a jet with super sound-velocity produced by a not too high excess-pressure is shown in fig. 9. The pitot-pressure close to the jet-hole is equal to the static pressure p_0 in the container. If the pitot-sound is gradually moved out along the axis of the jet, the reading of the pitot-manometer is seen to fall to a minimum, the position of which very nearly coincides with the point D_1 of fig. 3. Then again the reading increases to a maximum value of about p_0 close to the border-line A_1B_1, fig. 3, of

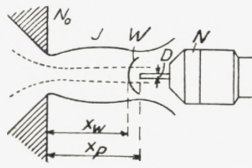

Fig. 8 b. Pitot-Apparatus with Sound.

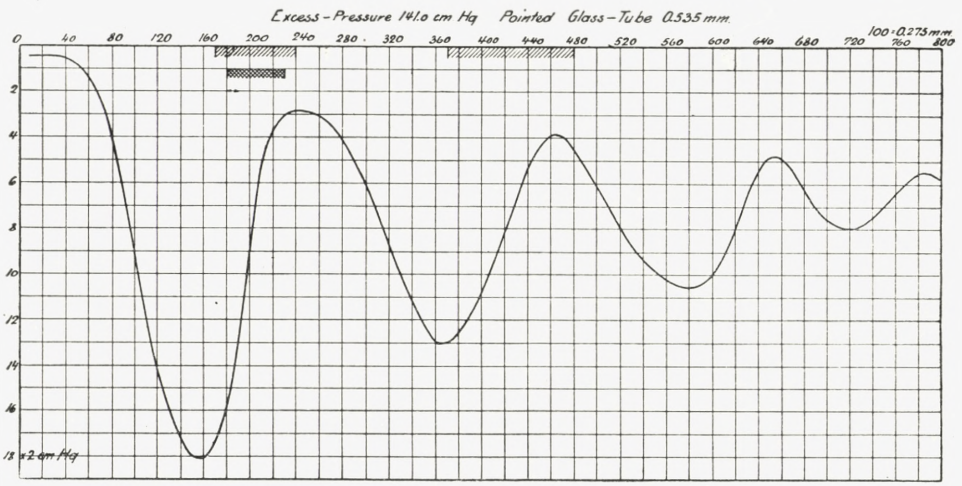

Fig. 9. Pitot-Curve. Ordinate: Difference between Pressure in Container p_0 and Pitot-Pressure p'_0.

the first jet-section, then falls off to a new minimum in the centre D_2 of the second section, rises to ab. p_0 in A_2B_2, and so on. In fig. 9 the abscissa represents the distance from the jet-orifice to the front of the pitot-sound indicated above. Later investigations carried out with pitot-sounds and nozzles of various dimensions revealed a general pro-

perty of the pitot-curve which throws a clear light on the nature of the same.

In photographs of the jet with the pitot-sound or the pitot-nozzle a compression-wave is seen, as might be expected from what has been stated in the preceding paragraph. The aspect and position of the wave varies with the character of the sound or nozzle about as indicated by S in fig. 8 a and b. With a nozzle the distance from the wave to the mouth of the pitot-apparatus is greater than with a thin sound. Generally the distance is the greater, the greater the dimension D. If now the pitot-curves were plotted with the distance x_p, fig. 10, to the front of the sound or nozzle as abscissa, the several pitot-apparatus used gave curves varying in position as indicated in fig. 10 by a, b.

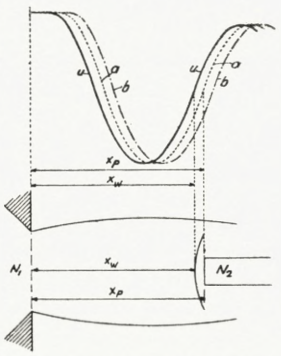

Fig. 10. Pitot-Curves a, b, obtained with different Nozzles N_2, all give the same reduced Curve u when the Position of the Compression-Wave is used as Abscissa.

If, however, instead of x_p the distance x_w to the central point of the compression-wave was taken as abscissa, all sounds and nozzles gave the same pitot-curve, say u in fig. 10. This is just what might be expected from the theory of the stoppage of the jet. At a given point of the central stream-line tube of the jet, say the point at the distance x from the jet-orifice, a given state of flow obtains. If a compression-wave perpendicular to the tube is in one way or other produced at this point, and the flow after having passed the wave is brought to a stand-still, then the pressure p'_0 at the point where the velocity is reduced to zero is solely determined by the state just in front of the wave, see equation 1, paragraph 4. Furthermore we have seen that

$\frac{p'_0}{p_0}$ could be expressed as a function of the ratio $\frac{p}{p_0}$ of the pressure p in front of the wave and the pressure p_0 in the container from which the jet is emitted. Obviously, then, a definite value of p'_0 corresponds to each point of the jet with its definite value of p. The said p'_0-value may be termed the stoppage-pressure of the said point, and what the pitot apparatus indicates is just the stoppage-pressure at that point of the central fibre of the jet where the compression-wave to which the pitot-apparatus gives rise is formed. The distance from the wave to the sound or nozzle of the pitot-apparatus is of no consequence. It is determined by the condition that there must be sufficient space for the air stopped by the sound or nozzle to escape laterally. Therefore, with a greater value of D, fig. 8 a and b, the distance must be greater than with a smaller value, as more air should be removed. From what has been said it will be understood that the pitot-curve should always be plotted with the distance to the compression-wave as abscissa, othervise it will depend on the special pitot-apparatus used in the determination of the curve. The curve thus plotted may be termed the normal pitot-curve.

6. Investigations on the Pitot-Curve.

The determination of the pitot-curve with the position of the compression-wave as abscissa must generally include photographing of the jet by the method of striæ in order to find the position corresponding to the reading of the pitot-manometer. In fig. 11 a—d, Pl. 2, a series of photographs from the determination of a pitot-curve are reproduced. The screen-edge of the apparatus of striæ, see fig. 20, was in these pictures perpendicular to the axis of the

jet. In fig. 12 a—b, Pl. 2, a similar series is seen. The screen-edge is again perpendicular to the axis, but it has been turned with regard to the direction of the flow. A pressure-gradient which appears dark in fig. 11 is therefore bright in fig. 12. The compression-wave in front of the pitot-sound is clearly seen, and it will be noted that the pressure-gradient behind the wave has, as should be expected, the opposite sign of the gradient just outside the nozzle from which the jet is emitted. In fig. 13 a—b, Pl. 3, the screen-edge was parallel to the axis of the jet. Finally in fig. 14 a—d, Pl. 3, a series of photographs from a determination of the pitot-curve by means of a nozzle like that of fig. 8 a is reproduced. The screen-edge is now again perpendicular to the axis of the jet. It will be noted that the compression-wave is found at a greater distance from the orifice of the pitot-apparatus, to the right, than in the case of an apparatus with a steel sound.

The experimental evidence of the fact stated above and preliminarily illustrated in fig. 10 is given in fig. 15. In the figure a series of pitot-curves are drawn, corresponding to various sounds and pitot-nozzles, see fig. 19. The abscissa is the position of the said sounds and nozzles. In connection with the pitot-readings photographs like those reproduced above were taken, after which each reading of the pitot-manometer was plotted against the distance from the jet-orifice to the compression-wave determined from the corresponding photograph. In this way the points to the left were found, clustering round a common curve, the normal pitot-curve.

Between the ordinates p'_0 of the normal pitot-curve and the static pressure p in the corresponding point of the jet the relation (2) in paragraph 4 obtains. It thus would seem

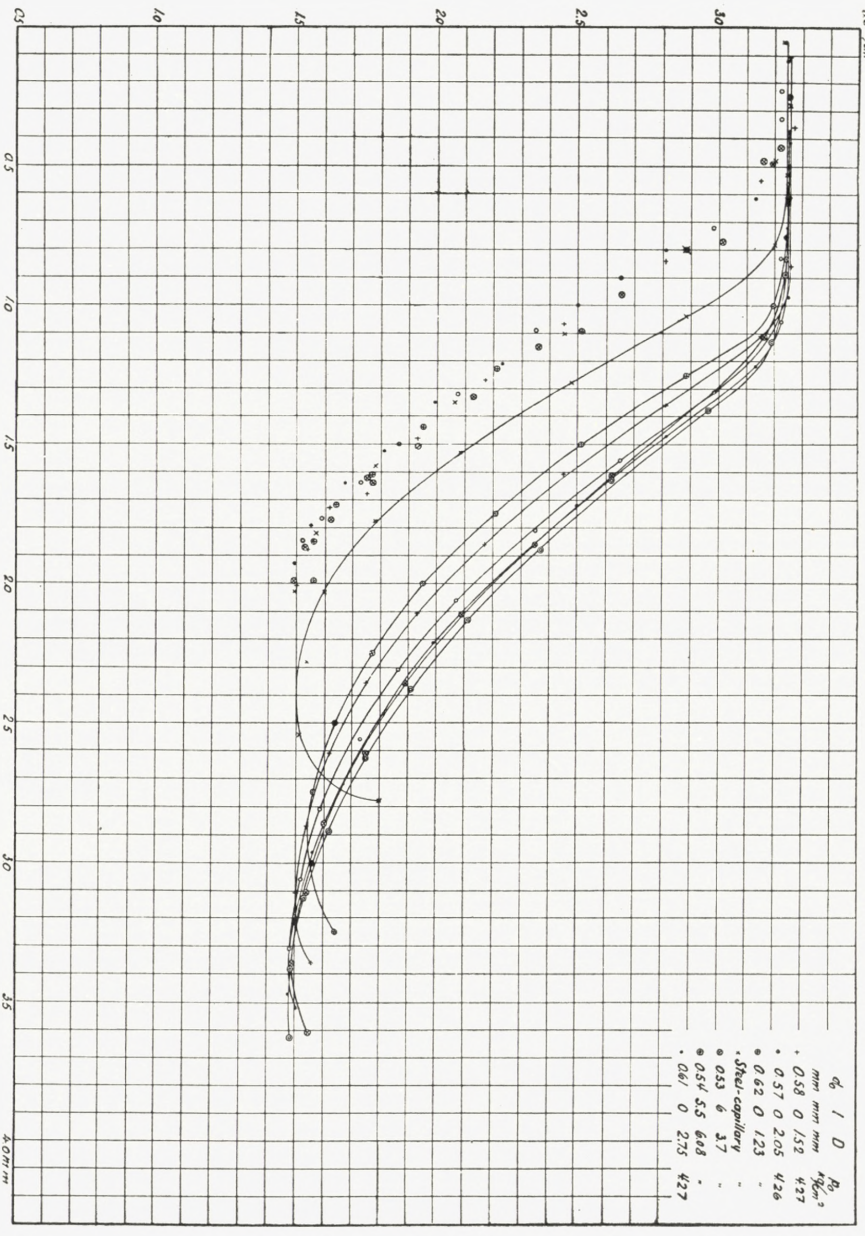

Fig. 15. Reduced Pitot-Curve determined by various Nozzles and Sounds.

possible to derive the static pressure curve from the pitot-curve for points along the axis of the jet. In fig. 16 the uppermost curve is a normal pitot-curve, while the lower represents the static curve calculated by means of the re-

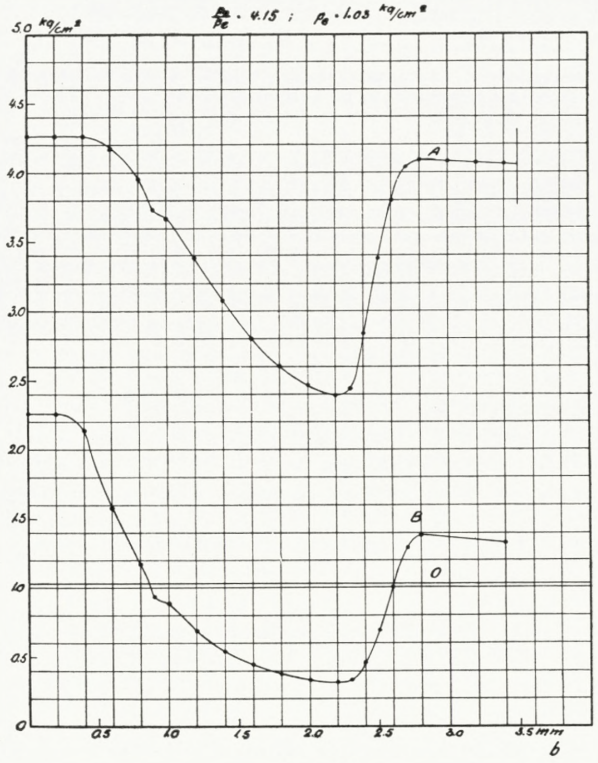

Fig. 16. Pitot-Curve *A* and corresponding Static Pressure-Curve *B*.

lation (2) referred to. It would have been interesting to check the calculated static curve by direct observation. Owing to the small dimensions of the jets it was, however, judged hopeless to try to obtain reliable observations by means of a static pressure gauge introduced into the axis of the jet.

Some investigations have been made on the distance $c = x_p - x_w$, fig. 10, from the compression-wave to the

pitot-sound or -nozzle. Results are given in fig. 17. The curve N was found with two nozzles of the type in fig. 8 a, while S originates from a tiny steel sound. The distance is, as indicated above, greater with the nozzle than with the sound. Furthermore it will be noted that the distance varies considerably along the axis. It is not even the same at two points of the same jet-section, for instance ABA_1B_1, fig. 3, with the same values of pressure and ve-

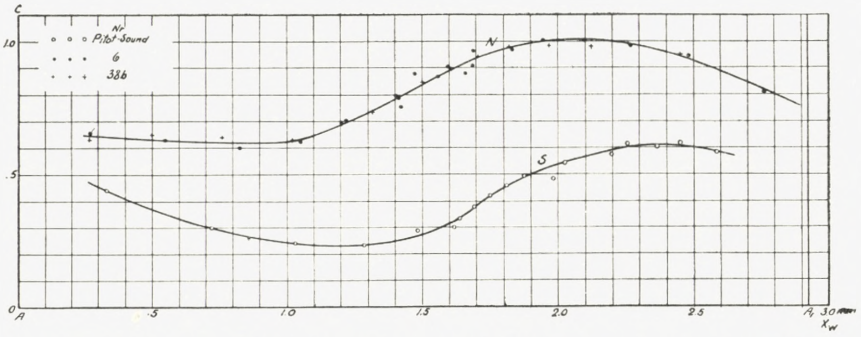

Fig. 17. Distance c between Compression-Wave and Pitot-Nozzle or Sound. N with Nozzle, S with Sound, Abscissa: Distance from Jet-Orifice to Compression-Wave x_w.

locity. Such points are generally found on either side of the point of minimum pressure, D_1, placed nearly symmetrically with regard to the latter point. With two symmetric points the distance c is smallest for the point nearest to the jet-orifice. The explanation is undoubtedly to be found in the circumstance that the velocity in the point nearest to the jet-orifice has an outward component, while in the symmetric point it has a component directed towards the axis of the jet. The radial component will pass unaltered through the compression-wave. For the point nearest to the jet-orifice the outward directed velocity-component will promote the escaping of the air behind the compression-wave, i. e. between the same and the pitot sound or

-nozzle. For the symmetric point the inwardly directed velocity will hamper the escape of the air. We should therefore anticipate just the variation of c shown in fig. 17, which figure covers the first jet-section ABA_1B_1. It may be noted that the radial velocity component φ_r is nearly maximum at distances from the jet-orifice equal to $^1/_4$ and $^3/_4$ of the length of the jet-section. As will be seen, the curves in fig. 17 exhibit the smallest and greatest values close to these points.

II

Investigations on the Modus Operandi of the Pulsator.

1. Experimental Arrangements.

In the investigations here described the air was supplied by a compressor operated by a 5 h. p. d. c. motor. The plant was furnished with an air-chamber of ab. 0.5 m^3 capacity. In the latter the excess-pressure was generally kept at 7—8 Atm. In fig. 18 a L indicates the main pipe from the compressor. To the outlet-stud with the valve V_1 the chamber C_1 (40 l) was attached with a view to roughly smoothing out variations in the pressure. From C_1 the air flowed through the reduction-valve R_1 to the nozzle N_J of the acoustic generator A, a second air-chamber, C_2, with a manometer M_1 being attached to the connecting pipe. The nozzle N_P of the pulsator was, through a flexible tube, connected to the pulsator proper, P, consisting of a steel-bottle of varying size. To the pulsator a manometer M_P was attached. Furthermore, in many experiments, the arrangement ab was used. By means of the latter a constant pressure could be kept in the pulsator during the filling, and so an arbitrary stage of the filling-process could be maintained for closer examination. The arrangement consists of two parallel branches through which the pulsator could be put in connection with the atmosphere. In one branch

a valve V_5 of large aperture in the other a screw-valve V_6 for fine adjustment of the flow was furnished. Furthermore a valve V_4 was provided for direct connection between P and the atmosphere.

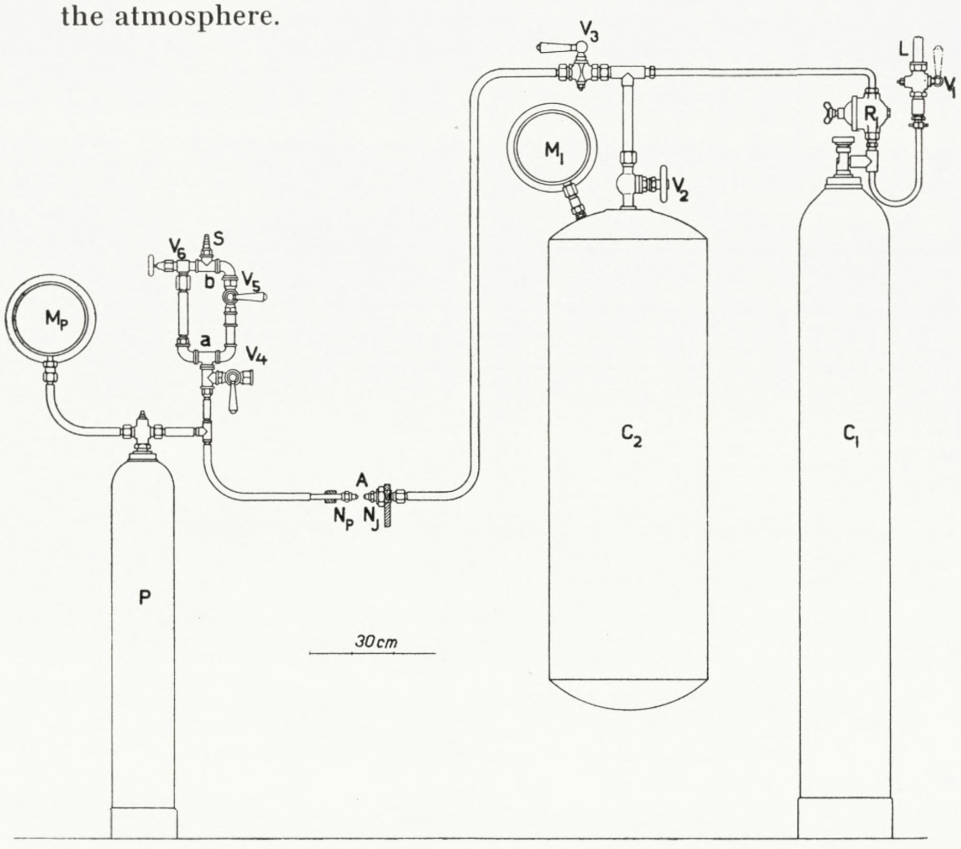

Fig. 18 a. Experimental Arrangement.

In certain experiments the flow of air to the pulsator was to be measured at an arbitrary stage of the filling-process. The arrangements for this are shown to the right in fig. 18 b. In a pipe L' connected to the stud S, fig. 18 a, a bore N was inserted between the two extensions B_1 and B_2. By means of the water-gauge M_3 the pressure-drop in N, to which the flow from the pulsator gave rise, was measured. A thermometer T was inserted in the lower

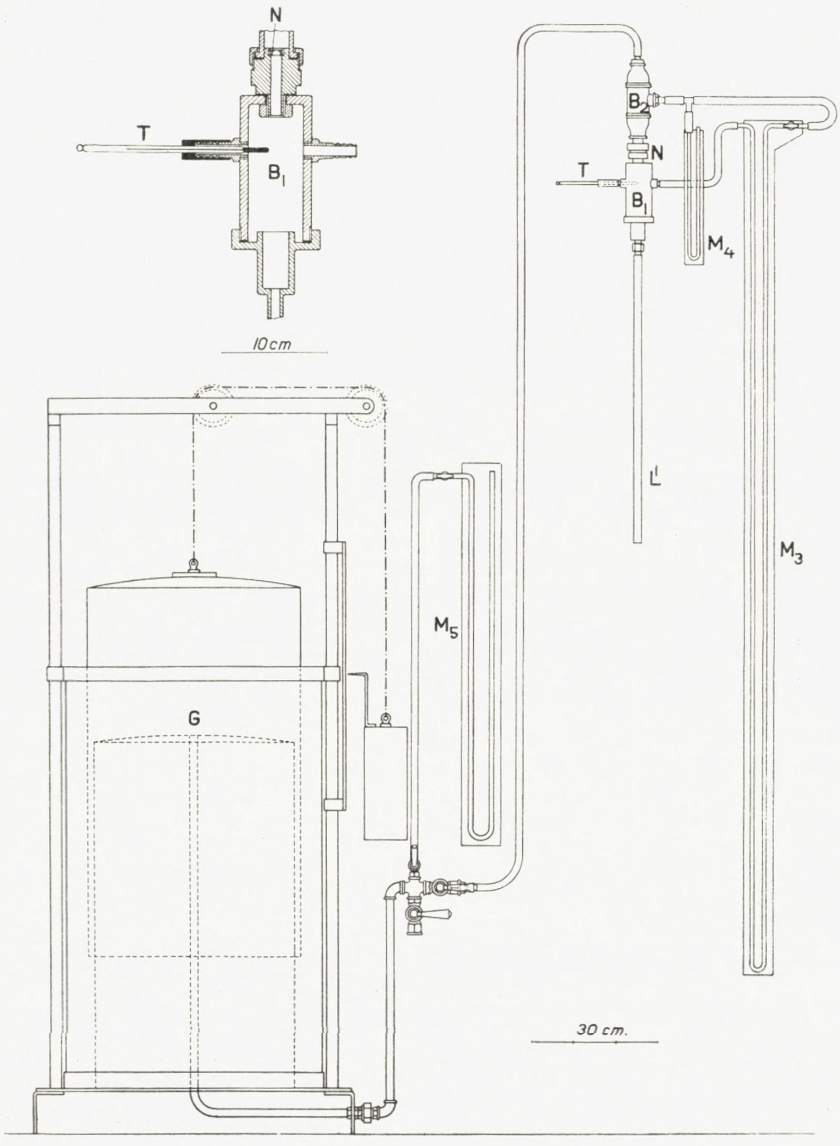

Fig. 18 b. Experimental Arrangement.

extension B_1 and a small water-gauge M_4 was connected to the uppermost extension B_2 in order to give the absolute pressure in B_2. From B_2 a pipe was carried to the gasometer G which was used either for direct determin-

ation of the flow or for testing the gauge M_3 as a flow-meter in connection with the arrangement B_1NB_2. The gasometer had a capacity of ab. 140 l.

A photograph of the acoustic generator is given in fig. 21, Pl. 4. The pulsator-nozzle is mounted on a triple slide

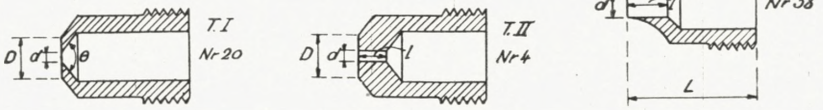

Fig. 19 a. Fig. 19 b. Fig. 19 c.

Fig. 19. Acoustic Generator. Nozzles.

arrangement. Various types of jet-orifices and pulsator-nozzles have been employed. Diagrams are shown in fig. 19 a—c and a list of all the orifices and nozzles is found under tab. II.

An indispensable means for the investigation was the optical apparatus used for the production of photographs

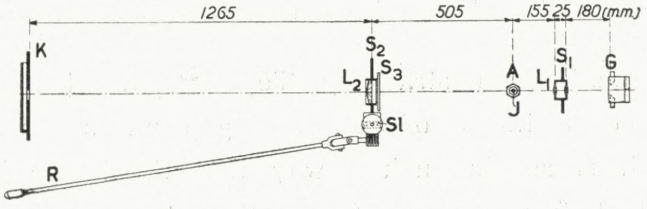

Fig. 20. Optical Arrangement.

according to the method of striæ. Fig. 20 shows the general arrangement. G indicates the spark apparatus, L_1 a lens mounted in a screen S_1, A the air-jet generator and J the jet proper. L_2 is a lens in a screen S_2, while S_3 is another screen in front of the lens and covering nearly half of it. Finally K is a holder for the photographic plate. As will be known from the description

Tab. II. List of Nozzles and Jet-Orifices

Type I, Fig. 19 a Obtuse conical.			Type II, Fig. 19 b Flat, cylindrical.				Type III, Fig. 19 c Pointed, cylindrical.		
No.	d	D	No.	d	D	l	No.	d	l
	mm	mm		mm	mm	mm		mm	mm
1	1.47	5.8	2	1.47	6.4	2.0	36 b	1.38	5
3	2.14	6.5	4	2.11	6.7	3.0	38 a	2.07	5
5	2.32	5.8	6	0.54	6.4	3.5	38 c	2.00	5
13	0.58	1.0	7	0.56	3.7	2.0	39	1.50	5
14	0.76	3.8	8	1.04	7.5	6.5	41	0.37	5
15	0.77	1.0	9	1.50	7.0	7.0	42	0.70	5
19 (Z I)	2.04	7.2	10	2.02	7.0	6.0	43	2.43	5
20 (Z II)	2.05	8.0	12	0.54	3.7	6.0	38 b	2.20	5
21 (Z III)	2.04	8.1	23	2.03	6.4	1.5			
22 (Z IV)	2.03	8.0	24	2.03	6.2	2.0			
29	0.61	2.7	25	2.03	6.5	1.5			
30	0.57	2.0							
31	0.58	1.5							
32	0.62	1.2							
33	0.52	5.5							
34	0.76	5.5							
35	1.05	5.5							
36 a	1.49	5.7							
37	2.02	5.4							

of the method of striæ by Töpler[20], the lens L_1 is to project an image of the spark-gap on to the screen S_3 which is set in such a way that the image is just screened off from the lens L_2. By the latter lens an image of the object to be photographed, i. e. in our case the air jet J, is formed on the photographic plate. The plate could be displaced in the holder K so that a series of pictures could be taken on the same plate. All parts of the arrangement are mounted on an optical bench in order to facilitate the various adjustments. It is essential that the edge of the screen S_3 can be set very accurately with regard to the image of the spark, and that the setting can be varied

from the position of the observer behind the frosted glass of the camera *K*. Hence a slide arrangement *Sl* to be moved by means of the rod *R* was furnished.

The electrodes of the spark-apparatus consisted of two strips of sheet-zink between two rectangular pieces of fuzed quartz. The thickness of the strips was ab. 0.5 mm, the length of the spark-gap 5—8 mm. The sparks were produced by means of an inductor of ab. 25 cm spark-length. In parallel to the gap 6 Leyden-jars of medium size were inserted. The front edges of the quartz pieces were covered with black enamel to make them intransparent. In this way a regular rectilinear light-source of great brightness was produced. In series with the spark-gap another variable gap was inserted so as to ensure that only one single spark was produced at each interruption of the inductor-current.

In fig. 21, Pl. 4, a photograph of the main parts of the optical arrangement, except the camera, is reproduced. The aggregate $L_2 S_2 S_3$, fig. 3, appears in the front-part of the picture. Behind, the acoustic generator is seen, the nozzle of the pulsator having been displaced by a cylindrical oscillator with its holder. In the rear of the generator is the lens L_1 with its screen and in the background of the picture the spark-gap apparatus is discerned. The quartz plates of the latter have, however, been temporarily removed. To the left are the Leyden-jars. The inductor may be dimly seen behind the latter.

2. Anticipations with Regard to the Explanation of the Pulsation-Process.

Before the investigations, described below, were commenced we had formed an idea of the modus operandi of the pulsator which may be illustrated by means of fig. 22.

Here N_1 indicates the jet-orifice and N_2 the mouth-piece of the pulsator. From N_1 an air-jet J is emitted, the pitot-curve of which is P_1. In the figure the mouth of the pulsator is placed inside the first interval of instability. Obviously the pulsator must fill with air, and it would seem reasonable to assume that it will charge to a pressure equal to the pitot-pressure i. e. the pressure indicated by the point c of the pitot-curve P_1 (especially if this curve were found by means of a pitot-sound identical with the nozzle of the pulsator). Now, it is easy to see that the state of the pulsator when charged to the said pressure cannot be a stable one. For any disturbance causing air to escape from the pulsator will undoubtedly set up a jet which at the outset will generally have a velocity higher than that of sound, thus a pitot curve P_2 of the same type as that of the main jet. As the curve P_2 will be above the curve P_1 out to the point a, the main jet will not be able to check the jet bursting forth from the pulsator within this distance from N_2. So it may be anticipated that the pulsator-jet will penetrate to a. As now the pulsator gradually empties, the pitot-curve falls, as indicated in the figure, while at the same time the front of the pulsator-jet retreats. It was thought likely that the discharge would continue down to the pressure at which the pitot-curve of the pulsator just touched the curve of the main jet. Then, at any rate, the state is again instable as the curve-

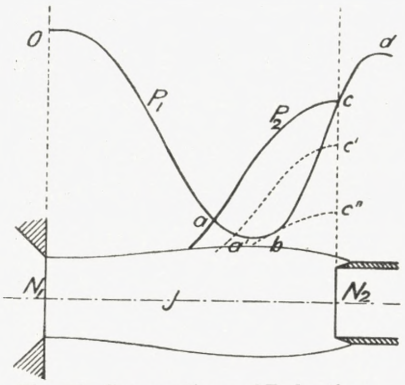

Fig. 22. Conception of Pulsation-Process. P_1 Pitot-Curve of Main-Jet, P_2 Pitot-Curve of Jet penetrating from Pulsator.

branch *bc* is at any point higher than *bc''*. So undoubtedly the main jet will burst forth to N_2 and recharge the pulsator.

It was the main object of this investigation to put the anticipations just indicated to the test and, if possible, to

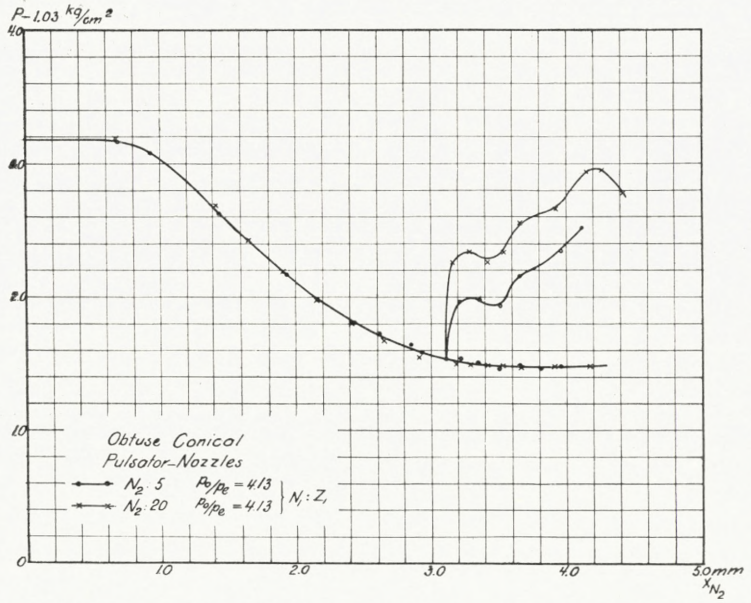

Fig. 23. Limits of Pulsator-Pressure during Pulsations with obtuse conical Pulsator-Nozzles. Abscissa: Distance x_{N_2} from Jet-Orifice to Pulsator-Nozzle. Ordinate: Excess-Pressure in Pulsator.

reveal the mechanism of the various parts of the pulsation-process.

3. Pulsator-Diagrams.

As a first step in the research-work it was found wise to investigate the limits between which the pressure in the pulsator P varies during the process of pulsation. With sufficiently slow pulsations the limits may simply be observed on a manometer M_p, fig. 18 a, applied to the pulsator.

If such observations are made, corresponding to a series of positions of the pulsator-nozzle, a diagram may be drawn from which an idea may be formed with regard to the effectiveness of the pulsator as a means of setting up pulsations. In order to find out the shape of pulsator-nozzle best suited for the purpose, a fairly large number of diagrams of the type indicated were produced. Some of them are shown in figs. 23—25. In the figures the distance x_{N_2} from the jet-orifice N_1 to the pulsator nozzle N_2 is taken as abscissa. The said holes

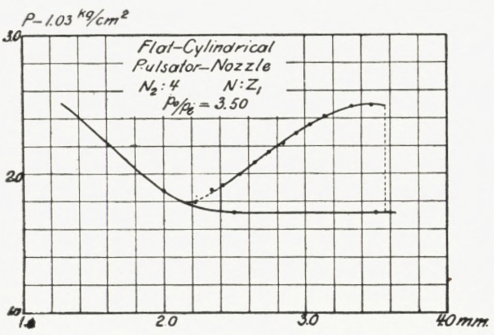

Fig. 24. Limits of Pulsator-Pressure during Pulsation with flat cylindrical Pulsator-Nozzle (Comp. Fig. 23).

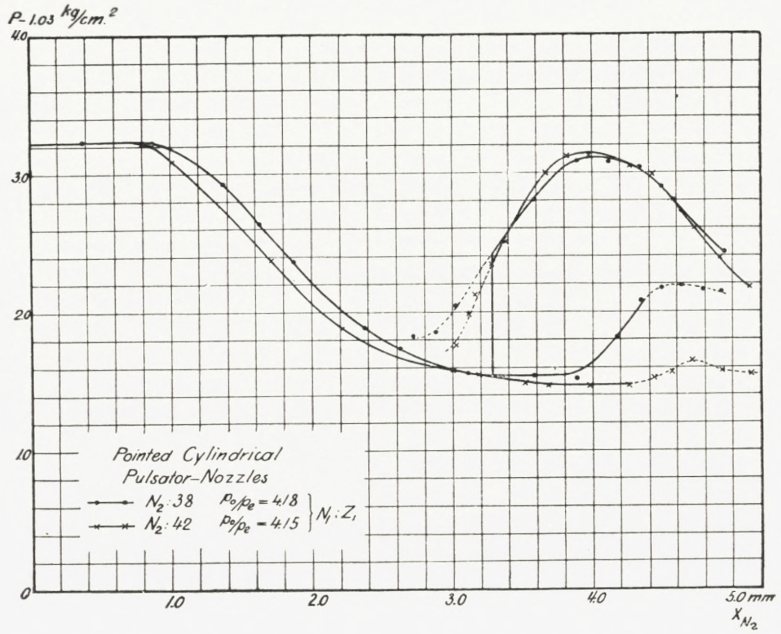

Fig. 25. Limits of Pulsator-Pressure during Pulsation with pointed cylindrical Pulsator-Nozzles. (Comp. Fig. 23).

and nozzles are characterized by the indications in tab. II. It is seen that the lower branch of the curves, representing the lower limit of the pressure in the pulsator, does not as a rule depend so much on the type of the pulsator-nozzle as the upper branch representing the upper limit of the pulsator-pressure. The lower limit of the pressure exhibits a tendency to keep constant throughout the interval of instability. The pointed pulsator nozzles seem, however, to form an exception from this rule in that the lower branch curves upwards, fig. 25. The upper branch is, as indicated, highly dependent on the type of the nozzle. It seems that pulsator-nozzles of the types *T II* and *T III*, fig. 19, with a cylindrical bore, furnish the most effective means for the production of vigorous pulsations. For not only is the upper limit high over the greater part of the interval of instability (fig. 24—25), but the limiting pressure also exhibits a high degree of definiteness. As a matter of fact this pressure repeated itself with an exactness practically equal to the certainty with which the manometer could be read, i. e. ab. 0.02 kg/cm^2,

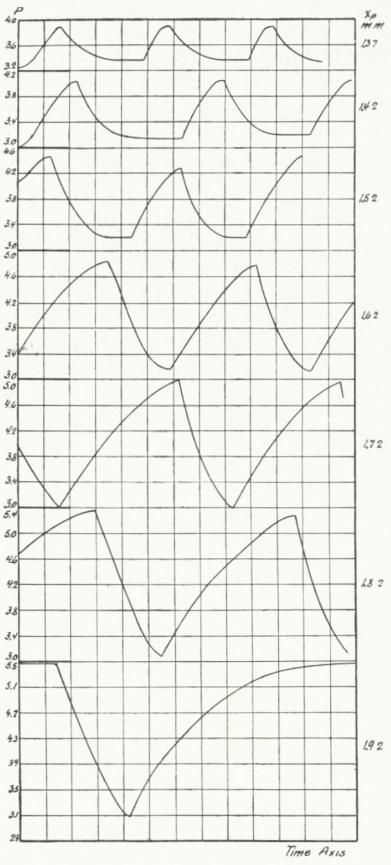

Fig. 26. Pulsator Oscillograms. Ordinate: Pressure in Pulsator. Abscissa: Time. Figures to the right: Distance x_p from Jet-Orifice to Pulsator.

while with flat conical nozzles, fig. 23, the uncertainty of the maximum pressure was as high as 0.1 kg/cm^2 or above.

In fig. 25 parts of the curves are drawn with a dotted line. Within the interval thus indicated the pulsations do not start automatically but could be started in a way explained in paragraph 5 below.

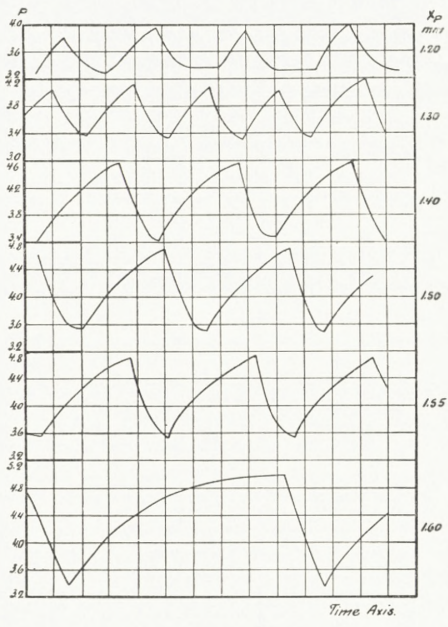

Fig. 27. Pulsator Oscillograms. (Comp. Fig. 26).

Complete "pressure-oscillograms" for the pulsator were taken in addition to the diagrams described above. With very slow pulsations the oscillograms were obtained by direct observation of the pressure at a number of instants of the period. With more rapid pulsations the oscillograms were produced by means of a Watt-indicator. In figs. 26 and 27 oscillograms of the latter descriptions are reproduced. The two parts of the pulsation-process, the filling and the exhaustion, are clearly distinguished. In the pictures the distance of the pulsator-nozzle from the entrance to the interval of instability is gradually increased. It is seen that with the pulsator-nozzle in the foremost part of the interval, the pulsations are comparatively small. The exhaustion is protracted and the time of exhaustion is in some degree lacking in definiteness, indicating that the instability at the end of the exhaustion is less pronounced. Farther

back in the interval the pulsations become more vigorous. The time of filling is generally longer than that of exhaustion, and the change from one part of the pulsation-process to the other takes place with great regularity. Finally, close to the exit of the interval the process of filling is protracted, and the setting in of the discharge becomes less definite in time. In the following the two parts of the pulsation-process are considered separately.

4. The Process of Discharge. Investigations by the Method of Striæ.

The most direct method of investigating the modus operandi of the pulsator is certainly that of the striæ. It was applied to the process of discharge. During the said process a series of instantaneous photographs were taken by means of the optical arrangement in fig. 20. Samples of such series are given in figs. 28—30, Pl. 4—5. In fig. 28 the lens-screen is perpendicular to the axis of the jet and so it is in fig. 29, but the direction of the jet relatively to the screen-edge has been changed. In fig. 30 the jet is parallel to the said edge. It is found that the pulsator-jet, at the start of the discharge, is quite suddenly shot out from the orifice of the pulsator. The jet is of the same character as that of the main jet, thus a jet with a velocity exceeding that of sound. In the collision between the two jets two compression waves, one in each of the jets, are formed. Between the two waves is a layer from which the air from the two jets escapes laterally. By following the progress of the process of discharge in the row of pictures, which corresponds to nearly equidistant moments, it is seen that the layer of collision remains for a good while

in almost the same spot. Later on during the process it is, however, forced back towards the pulsator-nozzle, to the left, by the main jet, owing of course to the decrease of the pressure in the pulsator. Finally the compression-wave in the pulsator-jet seems to disappear into the pulsator-nozzle. Notably it is always found apparently to do so with the nozzle in the foremost part of the interval of instability. Shortly after, the process of discharge is brought to an end by the sudden setting in of the process of charging.

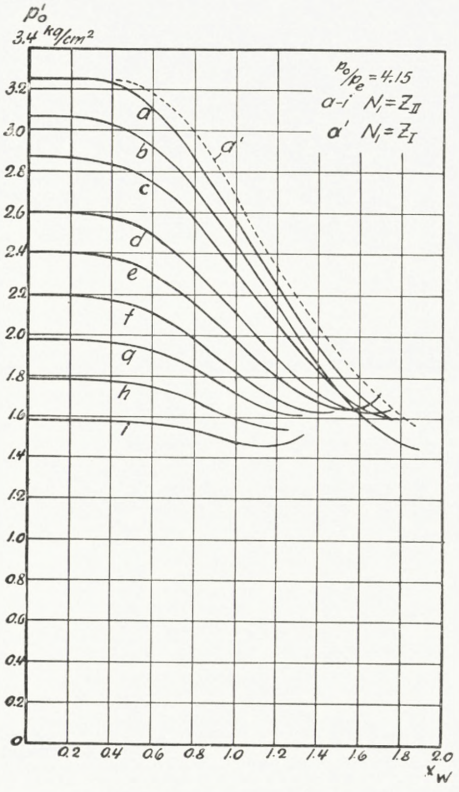

Fig. 31. Series of Pitot-Curves.

From the pictures it is seen how far the pulsator jet penetrates towards the jet-orifice. We should thus be able to test the anticipation in fig. 22 provided the pitot-curves for the main jet and the pulsator-jet were known with the pressures which obtain in the container and the pulsator.

In order to be able to carry out the test, series of pitot-curves corresponding to a considerable number of values of the ratio $\frac{p_0}{p_e}$ of the pressure in the container and the external pressure were determined for a number of nozzles used as jet-orifices and mouth-pieces for the pulsator. In the determination the pitot-apparatus was furnished

with a nozzle with a plane front-side of such an extension that it could be considered as a wall stopping the air-jet. A sample of a series of curves is given in fig. 31. Instantaneous pictures were taken along with the readings of the pitot-manometer so that the distance τ from the compression-wave to the pitot-nozzle could be measured. After this the material necessary for investigating the question of the position of the collision-layer and of the character of the said layer was at hand, and the very simple state of things illustrated in fig. 32 was disclosed.

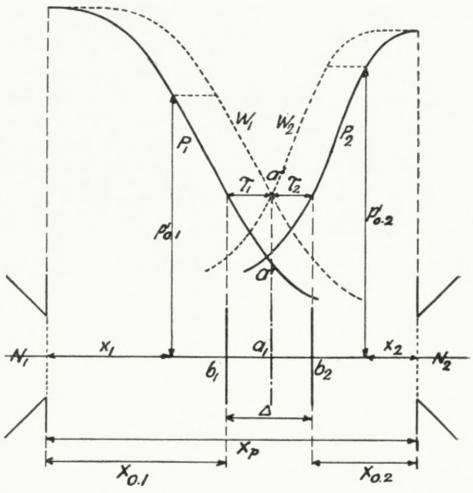

Fig. 32. Collision between two Jets with Velocities exceeding that of Sound.

Here P_1 and P_2 indicate the two pitot-curves corresponding to the pressures which obtain in the container and the pulsator at the moment considered. As explained in part I, an ordinate of the curves $p'_{0.1}$ resp. $p'_{0.2}$ represents the stoppage-pressure of the central stream-line tube when the flow of the latter is stopped through a perpendicular compression-wave at the corresponding distance (x_1 resp. x_2) from the nozzle in question. Now in fig. 32 two other curves W_1 and W_2 are drawn. They indicate the position of walls of infinite extension perpendicularly to the jets which in stopping the same would give rise to compression-waves at distances from the walls equal to the horizontal distances between the curves W_1 and P_1 respectively W_2 and P_2. The two curves W_1 and W_2 intersect each other at the point a and

in the corresponding point a_1 of the jet is the point of collision between the two jets, that is to say, the point where the two central stream-line flows meet and are brought to a stand-still. The two compression-waves are at the same time found at the points b_1 and b_2. The collision between the two jets thus takes place as if an infinitely thin wall were inserted between the two jets.

The statement given above implies that the width Δ of the layer between the two compression-waves of the collision is found equal to the sum of the two distances τ_1 and τ_2 at the points b_1 and b_2. In tab. III a comparison between Δ and $\tau_1 + \tau_2$ is undertaken. The agreement is practically perfect.

The statement illustrated in fig. 32 furthermore involves that the two compression-waves are found at points corresponding to the same pitot-pressure in the two jets. How exactly equal the two pressures are appears from the comparisons in tab. IV a—c in which P indicates the pressure in the pulsator and $p'_{0.1}$, $p'_{0.2}$ the pitot-pressures at the positions of the two compression-waves.

Tab. III.

τ_1	τ_2	$\tau_1 + \tau_2$	Δ
mm	mm	mm	mm
0.92	0.73	1.65	1.71
1.01	0.70	1.71	1.76
1.13	0.73	1.86	1.78
0.92	0.60	1.52	1.60
0.87	0.63	1.50	1.50
0.91	0.70	1.61	1.62
0.90	0.71	1.61	1.62
0.95	0.70	1.65	1.62
1.01	0.73	1.74	1.68
1.05	0.69	1.74	1.73
0.89	0.60	1.49	1.60

Tab. IV a.

$\frac{p_0}{p_e} = 4.15,\ x_p = 3.27$ mm.

P	$x_{0.1}$	$x_{0.2}$	$p'_{0.1}$	$p'_{0.2}$
kg/cm²	mm	mm	kg/cm²	kg/cm²
3.20	1.32	0.32	3.25	3.19
3.10	1.40	0.32	3.12	3.09
3.00	1.48	0.19	3.01	3.00
2.90	1.55		2.91	2.90
2.80	1.65	no	2.79	2.80
2.70	1.74	wave	2.69	2.70
2.55	1.84		2.60	2.55

Tab. IV b.

$\frac{p_0}{p_e} = 4.15,\ x_p = 3.78$ mm.

P	$x_{0.1}$	$x_{0.2}$	$p'_{0.1}$	$p'_{0.2}$
kg/cm²	mm	mm	kg/cm²	kg/cm²
3.3	1.45	0.83	3.07	3.04
3.2	1.45	0.80	3.06	2.99
3.1	1.48	0.74	3.00	2.95
3.0	1.50	0.66	2.98	2.92
2.9	1.53	0.58	2.93	2.85
2.8	1.65	0.48	2.80	2.79
2.7	1.74	0.27	2.70	2.70

Tab. IV c.

$\frac{p_0}{p_e} = 4.15,\ x_p = 4.23$ mm.

P	$x_{0.1}$	$x_{0.2}$	$p'_{0.1}$	$p'_{0.2}$
kg/cm²	mm	mm	kg/cm²	kg/cm²
3.7	1.48	1.13	3.00	3.04
3.5	1.55	1.06	2.91	2.98
3.3	1.57	1.00	2.89	2.91
3.1	1.62	0.93	2.82	2.81
2.9	1.67	0.83	2.77	2.76
2.7	1.77	0.59	2.66	2.68
2.6	1.84		2.60	2.60

When the pulsation-process has nearly come to an end, the compression-wave in front of the pulsator disappears, as already indicated, and now the jet emitted from the pulsator has a velocity smaller than that of sound. Now, with a jet the velocity of which is less than that

Tab. V a.

Jet-Nozzle Z I. Pitot-Nozzle No. 20 (Z II). $\frac{p_0}{p_e} = 4.16$.

x_p	$p'_{0.1}$	P
mm	kg/cm²	kg/cm²
2.80	1.90	1.92
—	1.81	1.82
—	1.77	1.74
—	1.68	1.68
—	1.63	1.63
3.00	2.07	2.07
—	1.91	1.92
—	1.81	1.80
—	1.73	1.70
—	1.61	1.61
3.20	2.19	2.15
—	1.99	1.99
—	1.91	1.90
—	1.74	1.73
—	1.56	1.57

of sound, the stoppage-pressure, i. e. the pitot-pressure, is simply that of the container from which the jet is emitted, barring the frictional losses in the bore. Hence, when the compression-wave in front of the pulsator disappears, it may be anticipated that the pitot-pressure at the place of the compression-wave facing the nozzle of the main jet, thus $p'_{0.1}$ above, should simply prove equal to the pressure P which obtains in the pulsator. This is

in fact found to hold good, as will be seen from table V a—c.

In later experiments it was found that any phase of

Tab. V b.

Jet-Nozzle Z I. Pitot-Nozzle No. 5. $\frac{p_0}{p_e} = 4.16$.

x_p	$p'_{0.1}$	P
mm	kg cm²	kg cm²
3.84	2.04	2.02
—	1.90	1.90
—	1.78	1.80
—	1.67	1.70
—	1.57	1.58

the process of discharge could be retained simply by supplying as much air to the pulsator as was emitted

Tab. V c.

Jet-Nozzle Z I. Pitot-Nozzle No. 36. $\frac{p_0}{p_e} = 4.15$.

x_p	$p'_{0.1}$	P
mm	kg cm²	kg cm²
3.44	1.66	1.67
—	1.57	1.60
—	1.51	1.53
3.52	1.65	1.65
—	1.56	1.60
—	1.50	1.54
—	1.49	1.53
3.62	1.71	1.70
—	1.60	1.60
—	1.49	1.53

from the same through a pipe with adjustable valve. The arrangement shown in fig. 18 was used with the necessary

alterations. Under these circumstances the accuracy with which the process of discharge could be studied was greatly increased. Certain anomalies were thereby disclosed.

It was thus found that with pulsator-nozzle No. 20 (Z II) there was a tendency to find $p'_{0.2}$ larger than $p'_{0.1}$. The differences would be as great as 0.14 kg/cm^2, while the certainty with which the manometers could be read was ab. 0.03 kg/cm^2. On the other hand, with pulsator-nozzle No. 5, $p'_{0.1}$ was found slightly, say 0.06 kg/cm^2, in excess of $p'_{0.2}$ if the pulsator pressure was high. Finally with the pointed nozzle No. 38 the agreement between $p'_{0.1}$ and $p'_{0.2}$ was practically perfect.

A scrutiny of the corresponding photographic pictures showed that when $p'_{0.2}$ was found larger than $p'_{0.1}$ then the air from the collision-layer was found to bend towards the pulsator-nozzle somewhat in the shape of an umbrella partly covering the said nozzle. In cases where $p'_{0.1}$ was found higher than $p'_{0.2}$, the opposite state of things obtained in that the layer was now driven towards the nozzle of the main jet. With the pointed pulsator-nozzle No. 38 the air from the collision layer escaped laterally, leaving the free atmosphere access to the two jets. It was concluded that the discrepancies observed were due to the covering of the one or the other jet by the air from the collision-layer, because, when such covering takes place, the jet is not emitted into the free atmosphere. This means that the observed value $\frac{p_0}{p_e}$ of the internal and external pressures is too high and, again, that the values of $p'_{0.1}$ or $p'_{0.2}$ derived from the pitot-curves corresponding to the observed value of $\frac{p_0}{p_e}$ are too high.

5. The lower Reversion-Point.

The process of discharge generally comes to an end quite abruptly without any warning and while a considerable flow of air is still emitted from the pulsator. The question is what causes this sudden reversal from a discharge to a charging of the pulsator. It was thought

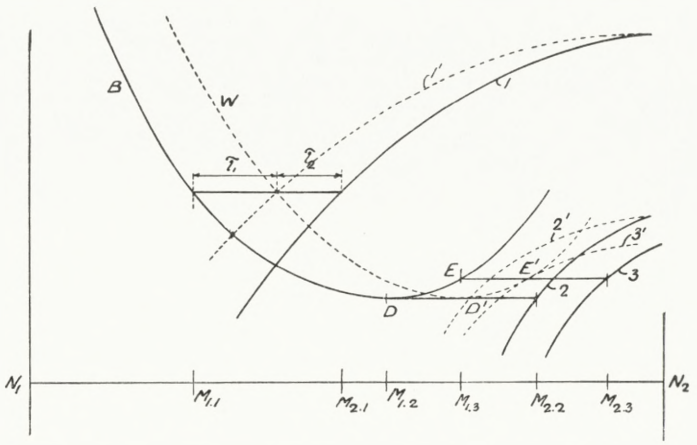

Fig. 33. Explanation of Reversion from Discharge to Filling.

likely that the phenomenon could be explained by the facts revealed in the preceding paragraph.

We may follow the process of discharge from its beginning by means of a diagram like that in fig. 32. At the start the layer of collision is formed between the two compression-waves $M_{1.1}$ and $M_{2.1}$, fig. 33. We shall now assume that during the following fall of the pressure in the pulsator the positions of the said layer may at any stage be determined in just the same way as at the first moment. That is to say, we shall assume the process of collision to be a quasi-stationary process, and we are undoubtedly justified in doing so because the said layer travels with a

velocity which, with a pulsator, is generally extremely small compared to the velocity of the two jets involved. (Conditions are undoubtedly different with the very rapid oscillations which may be set up by means of a small cylindrical oscillator. We are, therefore, not justified in applying the results of the investigations here recorded to the said oscillations without a special test, although it seems likely that the oscillations and the pulsations are related). During the process of discharge the compression-wave of the main jet will finally reach the lowest point D of the pitot-curve of this jet, for it is not to be seen what should stop the process of discharge before the said position is reached. The question is what will now happen. At the said stage the pitot-curve of the pulsator jet is 2, and the corresponding dotted curve 2′, representing the position of a fixed wall stopping the jet as described above, is just cutting the dotted curve W of the main jet at its minimum point D'. The pitot-curve of the pulsator-jet proceeds to fall, but still for some time the corresponding dotted curve will cut W, and it may therefore be anticipated that the compression-wave of the main jet may proceed beyond D and probably to the point E. The latter point is determined by the dotted curve 3′ of the pulsator-jet just touching W. What now happens with a further fall of the pressure in the pulsator is undoubtedly a little obscure. Most likely the discharge is practically checked at the moment E is reached. At any rate it cannot be long before the pulsator-jet is no longer able to produce a pressure large enough to resist the pressure of the main jet. Thus in a case like that in fig. 33, that is to say, in a case in which the pulsator-jet exhibits super-sound velocity during the whole process of discharge, E is probably very

nearly the point at which the compression-wave of the main jet stands at the last moment of the process of discharge.

Simpler relations obtain if the pulsator-jet, during the last phase of the said process, has become a jet with a velocity smaller than that of sound. In this case the compression-wave of the main jet will in all probability proceed to the point *D* and not beyond the same. It will be there at the moment the pressure in the pulsator has sunk to the pitot-pressure given by the ordinate of *D*. At that moment there will be equilibrium between the said pressure and the stoppage-pressure of the pulsator-jet, which pressure is just the pressure in the pulsator. Any further small discharge of the pulsator will now lower the stoppage-pressure of the pulsator-jet. But this means that the latter can no longer resist the main jet, as the stoppage-pressure of this jet can never sink below the minimum ordinate at *D*. The process of charging must therefore undoubtedly set in when the compression-wave of the main jet has reached *D*.

In addition to the discussion stated above certain anticipations with regard to the front of the interval of instability were formed.

If the nozzle of the pulsator is carried forward so that the compression-wave in front of this nozzle is formed inside that part of the main jet for which the pitot-curve falls, then we must undoubtedly expect the pulsator to charge to a pressure identical with the ordinate of the pitot-curve at the place of the compression-wave. Or rather, we know from the experiments recorded in part I that it is so. A discharge of the pulsator is out of the question. For if such a discharge were started, the compression-wave would be driven backwards towards the

nozzle of the main jet, that is to say, towards higher ordinates of the pitot-curve. So higher pressures would be created, opposing the outflow from the pulsator. And the outflow would therefore at once be checked. If now the nozzle of the pulsator is carried backwards away from the jet-orifice, the compression-wave will follow till it has reached the minimum-point of the pitot-curve. If the distance from the jet-orifice to the pulsator is made still greater than corresponding to this position of the compression-wave, the latter should come on the rising branch of the pitot-curve, provided a stable charging of the pulsator were possible. But, as already explained, it is not. So we must in all probability expect the front of the interval of instability to be that position of the pulsator which causes the compression-wave to fall in the minimum point of the pitot-curve.

A test on the anticipations stated above is now described. It included observations on the position of the compression-wave in the main jet at the last moment of the discharge. At the same time observations of the lowest pressure in the pulsator were taken with a view to comparing this pressure with the pitot-pressure corresponding to the said position of the compression-wave in cases where the two pressures were likely to coincide.

Attempts were made to find the final position of the compression-wave in question by making the process of discharge steady — at the last moment of the discharge — in the way indicated above. The scheme was, however, found difficult to carry out because just at the said moment a slight change in the pulsator-pressure gives rise to a comparatively great displacement of the compression-wave considered. So it was decided to try to find

the position by means of a photograph of the jet taken during the last part of the process of discharge in the illumination of a series of sparks of comparatively large frequency, say 20—30 per sec. The problem was to take the picture in such a way that the front of the wave in its last position could be discerned. This was no easy matter for the said front is partly covered by the pictures of the preceding waves. The movable screen S_3 of the optical arrangement, fig. 20, was therefore set so as to take away most of the light, leaving practically only a picture of the wave proper. This can be done because the refraction in the wave is so much larger than in the remainder of the jet. At the same time the photographing was started as late as possible. From the picture the position of the front of the last wave was found by adding to the distance x_0, fig. 34, from the nozzle of the main jet to the nearest wave the width Δ of the band of wave pictures, the said width being measured at the edge of the band where the waves appear practically without any extension in the direction of the jet,

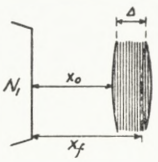

Fig. 34. Determination of the Wave-Front at the last Moment of the Process of Discharge.

We now pass on to consider the results. With an obtuse conical pulsator-nozzle of the type I (No. 20) it was found that the pressure P of the air in the pulsator at the last moment of the process of discharge, i. e. the lower reversion-point, was equal to the pitot-pressure in the main jet at the entrance to the interval of instability. This is true with all positions of the pulsator-nozzle inside the interval of instability, barring positions quite close to the exit-boundary of the interval where the pulsator-pressure grew rapidly with the distance from the jet-orifice.

Furthermore it was found that the point to which the compression-wave nearest to the jet-orifice advanced during the process of discharge was just the position of the wave in the main jet when the pulsator-nozzle was placed at the foremost limit of the interval of instability. This applies to all positions of the pulsator-nozzle N_2 for which the lower pulsator-pressure P_l was constant, compare fig. 23—25 and fig. 35, thus over the greater part of the interval of instability. In the rear of the latter, where the pulsator-pressure increases, it was observed that the compression-wave did not stop at the position corresponding to the entrance to the interval of instability but proceeded beyond the said position at a great rate.

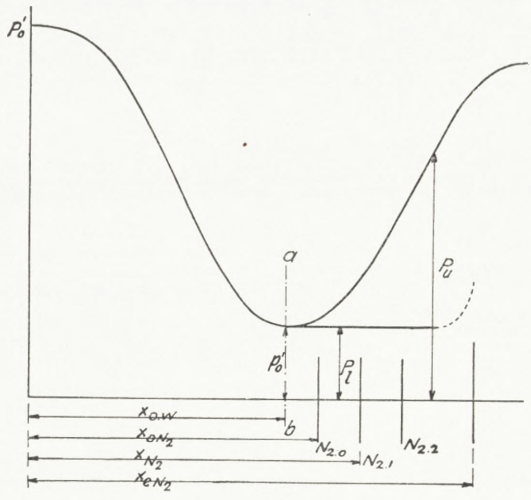

Fig. 35. Results of Investigation of the lower Reversion-Point.

The velocity of the motion was, as a matter of fact, so large that the consecutive positions of the wave were distinctly separated in the photograph, produced, as indicated, by means of a series of sparks with a frequency of 20—30 per sec. The results are illustrated in the diagram fig. 35, where *ab* is the position of the compression-wave in front of the pulsator-nozzle N_2 when the latter is placed just in front of the interval of instability at $N_{2.0}$. It will be seen that the main results agree with the anticipations stated above, provided the position *ab* coincides with the minimum of the pitot-curve. It very nearly does, as will

appear from fig. 36 in which the position, *ab*, has been marked. But otherwise it proved very difficult to locate the entrance to the interval of instability characterized by *ab* exactly in relation to the minimum-point because the determination of the latter point is very uncertain. This is due to the fact that the pitot-pressure just at the minimum-point varies extremely rapidly over the cross-section with a very pronounced minimum in the axis.

In the tables VI a—b samples of observations are given confirming the preceding statement with regard to the position of the compression-wave W_1 of the main jet in the lower reversion-point. In the tables VII a—b the constancy of P_l, i. e. the lower pressure in the pulsator, is illustrated.

All that has so far been stated in the present paragraph has, as will be noted, exclusive reference to the relations with an obtuse conical pulsator nozzle. With a cylindrical nozzle of types II or III certain anomalies are observed. In the first instance the interval of instability has no definite foremost boundary. Thus with a nozzle of type II, that is to say, a nozzle with a cylindrical bore and a flat front side, the compression-wave appeared less sharply within a certain region in front of the interval of instability. At the same time a slight movement of the pointer of the pulsator-manometer was observed, indicating a lack of stability in the state of the system. With a nozzle like that of type III, i. e. pointed with a cylindrical bore, the position of the compression-wave within a similar region in front of the interval of instability was very unstable. By means of a Kundt-tube is was found that acoustic oscillations were emitted from the nozzle

Tab. VI a—b.

$N_1 = Z_1$, N_2 = No. 20 $\frac{p_0}{p_e} = 3.50$ $x_{0.W} = 1.58$ mm (Fig. 35) $x_{0.N_2} = 2.48$ mm — $x_{e.N_2} = 3.80$ mm —		$N_1 = Z_1$, N_2 = No. 20 $\frac{p_0}{p_e} = 3.95$ $x_{0\,W} = 1.83$ mm (Fig. 35) $x_{0.N_2} = 2.84$ mm — $x_{e.N_2} = 4.20$ mm —	
x_{N_2}	x_W	x_{N_2}	x_W
mm	mm	mm	mm
2.52	1.62	2.92	1.87
2.62	1.67	3.07	1.91
2.72	1.69	3.22	1.87
2.77	1.64	3.37	1.89
2.87	1.70	3.52	1.89
2.97	1.68	3.67	1.81
3.07	1.72	3.82	1.81
3.17	1.65	3.97	1.81
3.27	1.58	4.17	1.87
3.37	1.58		
3.47	1.60		
3.57	1.58		
3.67	1.56		
3.77	1.60		

$x_{0.W}$ Position of Wave W_1 with Pulsator at the Entrance-Boundary of Interval of Instability.
$x_{0.N_2}$ Position of Pulsator-Nozzle when in Entrance-Boundary of Interval of Instability.
$x_{e.N_2}$ Position of Pulsator-Nozzle when in Exit-Boundary of Interval of Instability.
x_{N_2} Arbitrary Position of Pulsator-Nozzle.
x_W Corresponding Position of Wave W_1 in the Reversion-Point.

with a frequency corresponding to the natural period of the cylindrical bore acting as an open organ-pipe. In addition irregularities in the motion of the compression-wave could be directly discerned. Finally it was found that with nozzles of type III the pulsations only started when already of a comparatively large amplitude. If, how-

Tab. VII a—b.

$N_1 = Z_1$, $N_2 =$ No. 20 $\frac{p_0}{p_e} = 3.50$ $x_{0.N_2} = 2.48$ mm, $x_{e.N_2} = 3.79$ mm				$N_1 = Z_1$, $N_2 =$ No. 1 $\frac{p_0}{p_e} = 3.50$ $x_{0.N_2} = 2.50$ mm, $x_{e.N_2} = 3.74$ mm			
x_{N_2}	x_W	P_l	P_u	x_{N_2}	x_W	P_l	P_u
mm	mm	kg/cm²	kg/cm²	mm	mm	kg/cm²	kg/cm²
				2.50	1.61	1.72	
2.48	1.59	1.70		2.54	1.61	1.72	1.74
2.49	1.59	1.70	1.88	2.64	1.61	1.72	1.79
3.24	1.53	1.70	2.47	2.89	1.65	1.72	2.02
3.79		2.48		3.14	1.57	1.74	2.29
				3.39	1.65	1.74	2.47
				3.74	2.98	2.47	

ever, the aperture of the pulsator was for a moment partly shielded against the main jet, the pulsations would start with a position of the pulsator-nozzle closer to the jet-hole and with a correspondingly smaller amplitude. (Compare paragraph 3 and fig. 25).

Now in spite of the lack of definiteness indicated above and of the fact that the pulsator-pressure does not generally exhibit any definite final value before the pulsations set in, there is, as a rule, a rather definite and constant minimum value P_l of the pressure in the pulsator throughout the greater part of the interval of instability just as with the pulsator-nozzle of type I. And it should be noted that the said value does not seem to depend on the pulsator-nozzle, it being the same for all nozzles in combination with the same jet. Likewise it was found that the position of the compression-wave facing the jet-orifice in the lower reversion-point was also constant throughout most of the interval of instability, depending only on the jet and not on the pulsator nozzle. The tables VIII a—e are to illus-

trate the behaviour of cylindrical nozzles. In the tables (and in the tables VII a—b) P_u means the pulsator-pressure at the uppermost reversion point of the pulsation-process, comp. fig. 35. In the x_W column (—) indicates that no definite final position of the compression-wave W_1 could be

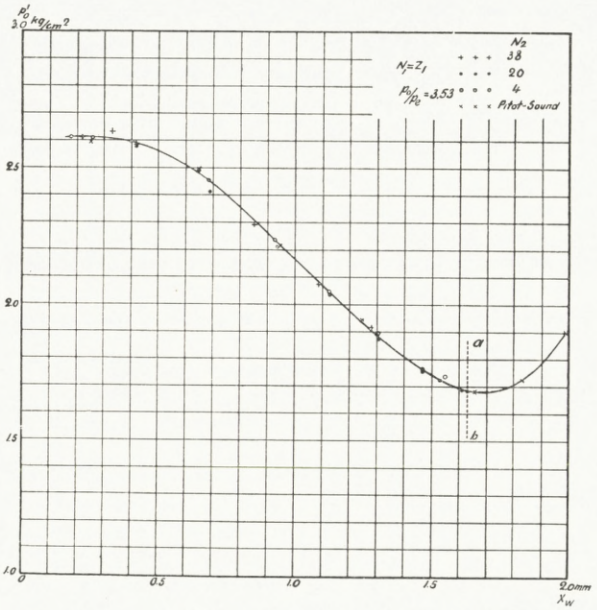

Fig. 36. Pitot-Curve with the Front of the Interval of Instability, *ab*, marked.

observed. The first value of x_{N_2} in each table represents the first position of the pulsator nozzle with which pulsations were obtained, thus the entrance to the actual interval of instability, while the last value indicates the exit-boundary of the said interval.

6. The Process of Filling.

While the shape of the pulsator-nozzle does not play any great part in the process of discharge and especially

Tab. VIII a—e.

$N_1 = Z_1$, $\frac{p_0}{p_e} = 3.50$					$N_1 = Z_1$, $\frac{p_0}{p_e} = 3.49$				
N_2	x_{N_2}	x_W	P_l	P_u	N_2	x_{N_2}	x_W	P_l	P_u
	mm	mm	kg/cm²	kg/cm²		mm	mm	kg/cm²	kg/cm²
No. 4 Tab. VIII a	2.42	1.65	1.72	1.91	No. 4 Tab. VIII c	2.34	1.56	1.73	1.87
	2.72	1.65	1.72	2.11		2.54	1.58	1.73	1.99
	3.02	1.61	1.72	2.34		2.74	1.62	1.73	2.15
	3.32	1.69	1.75	2.48		2.94	1.60	1.73	2.29
	3.47	(—)	2.32	2.49		3.14	1.60	1.75	2.41
	3.57	2.86	2.48			3.49	(—)	2.19	2.47
						3.54	2.82	1.46	
No. 2 Tab. VIII b	2.53	1.61	1.70	1.77	No. 38 c Tab. VIII d	2.55	1.60	1.72	1.91
	2.88	1.61	1.72	2.04		2.70	1.58	1.71	1.98
	3.18	(—)	1.85	2.37		2.85	1.58	1.71	2.10
	3.48	(—)	2.24	2.47		3.00	1.58	1.71	2.21
	3.58	(—)	2.47			3.15	1.58	1.71	2.31
						3.30	1.56	1.71	2.39
						3.40	(—)	1.87	2.46
						3.50	(—)	1.94	2.49
						3.60	(—)		2.48
					No. 40 Tab. VIII e	2.61	1.60	1.70	1.84
						2.76	1.60	1.70	1.93
						2.91	1.62	1.70	2.07
						3.21	1.58	1.70	2.35
						3.36	1.60	1.70	2.46
						3.46	1.62	1.70	2.47
						3.51	2.61	1.70	2.46

is without influence on the final pressure in the pulsator during the said process, it turns out that the character of the nozzle is quite predominant with regard to the value to which the pressure rises in the pulsator during the filling and also with respect to the regularity with which the process of filling repeats itself. It was found that, as already stated in paragraph 3, nozzles with cylindrical bores, whether flat or pointed, produce by far the most

vigorous pulsations and that the definiteness of the upper limit of the pulsator-pressure is with such nozzles astonishingly high. On the other hand, it turned out that obtuse conical nozzles, which exhibited well defined relations at

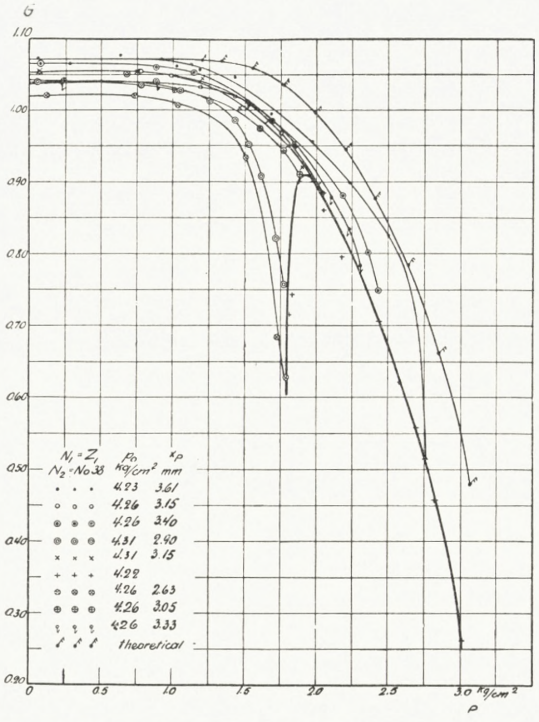

Fig. 37. Process of Filling. Abscissa: Pressure in Pulsator. Ordinate: Rate of Filling.

the lower reversion-point, give rise, at the upper reversion-point, to great irregularities in the completion of the process of filling.

In the study of the process of filling the rate of filling was first examined. Records hereof were already obtained in the pulsator oscillograms figs. 26 and 27. It is seen that the rate with which the pressure rises during the filling decreases as the counter-pressure in the pulsator increases. As, however, the temperature of the air in the pulsator

rises during the filling, the oscillograms are not suited for a determination of the mass of air G which flows into the pulsator per second.

With a view to measuring G directly, the pressure in the pulsator was kept constant by tapping off air at the rate of the filling. The air was collected in a gasometer, fig. 18 b, and so measured. In this way curves representing the variation of G during the process of filling were obtained. Samples corresponding to a series of positions of the pulsator-nozzle are given in fig. 37 where the abscissa is the counter-pressure P in the pulsator. It is seen that with small values of the pressure in the pulsator, G is independent of the said pressure just as is the rate of flow from one container into another through a bore when the ratio of the pressures is above the critical value, i. e. the value at which the velocity in the bore has become that of sound. With a view to comparison the curve, the uppermost, representing the flow determined by St. Venant's formula

$$G = S \cdot \sqrt{\frac{2\varkappa}{\varkappa - 1} p_0 \varrho_0 \left(\frac{P}{p_0}\right)^{\frac{2}{\varkappa}} \left(1 - \left(\frac{P}{p_0}\right)^{\frac{\varkappa - 1}{\varkappa}}\right)}$$

is drawn. The latter formula is known to hold good for the flow of an ideal gas between the two pressures p_0 and P through a hole of aperture S provided $\frac{P}{p_0} > 0.527$ and subject to the condition that S is and remains the smallest cross-section of the flow. With the pulsator-nozzle at greater distances from the entrance to the interval of instability the filling of the pulsator obviously takes place approximately as if the pulsator was connected with the air-container through a simple obtuse conical bore.

The curve drawn with a heavy line connecting the ends

of the G—P-curves represents, as will be understood, the rate of flow and the pulsator-pressure at the upper reversion-point. Or rather, it represents G corresponding to a pulsator-pressure ab. 0.01 kg/cm^2 below the pressure at the said point. So close to the reversion-point the flow could be made steady, and G measured with a cylindrical pulsator-nozzle.

7. The upper Reversion-Point.

The process of filling generally changes into the process of discharge as abruptly as the latter process is replaced by the former. In order to throw light on the process of filling and on the upper reversion-point, series of instantaneous photographs were taken. In fig. 38 a—c, Pl. 6, a sample is given. Fig. 38 a shows the jet at the beginning of the filling, fig. 38 c at the end, and fig. 38 b at an intermediate point of the process. At the first stage the jet seems to penetrate without hindrance into the pulsator-nozzle to the right. Later on a compression-wave appears in front of the same. The distance from the nozzle to the wave gradually increases till the upper point of reversal is reached. On the basis of the insight thus obtained the following conception of the cause of the sudden start of the discharge was formed.

As during the filling the pressure in the pulsator is increased beyond the critical value disclosed in fig. 37, the air in the pulsator acts more and more as a hindrance to the main jet and accordingly sets up a compression-wave in front of the pulsator nozzle. The said wave develops gradually as the static pressure in the pulsator and in front of the nozzle increases. At the same time more and more air escapes laterally. In this state of affairs no essential

change can take place before the static pressure in the pulsator has risen to the least stoppage-pressure occurring in any of the stream-line tubes of which the main jet consists. Generally the stoppage-pressure will be least for the central stream-line tube. It is therefore to be anticipated that the flow of the latter is stopped while the surrounding

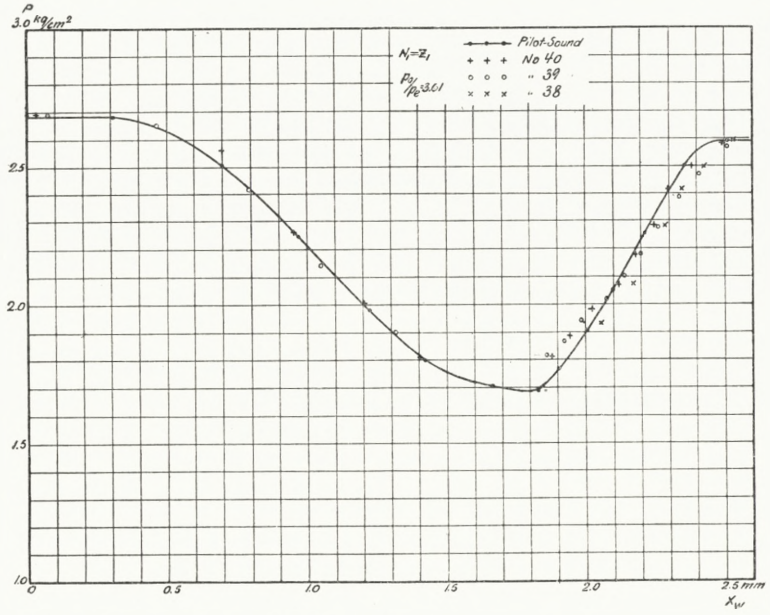

Fig. 40. Experimental Test of Conception with Regard to upper Reversion-Point.

tubes, owing to their larger stoppage-pressures, are not yet brought to a stand-still and so will continue to charge the pulsator. This state, however, can only last for quite a short moment, for owing to the said charging, the increase of the pressure in the pulsator will naturally cause a discharge from the pulsator along the central stream-line tube which cannot stand a larger pressure than its own stoppage-pressure.

With a view to testing the conception now indicated simultaneous observations of the pulsator-pressure and the

position of the compression-wave were undertaken at the upper point of reversal. From pitot-curves for the main jet the pitot-pressure corresponding to the said position of the wave could hereupon be found and compared with the pulsator-pressure. The final position of the wave was found by photographing the jet in the illumination of a series of sparks just as with the corresponding determination with the lower reversion-point. Now, however, the difficulties met with in the latter case were no longer present as the front of the wave is now also the front of the motion. Samples of the pictures are given in fig. 39 a—b, Pl. 6. It should be noted that the wave nearest to the jet-hole has nothing to do with the phenomenon here considered as it represents the wave which stops the jet from the pulsator at the first moment of the discharge.

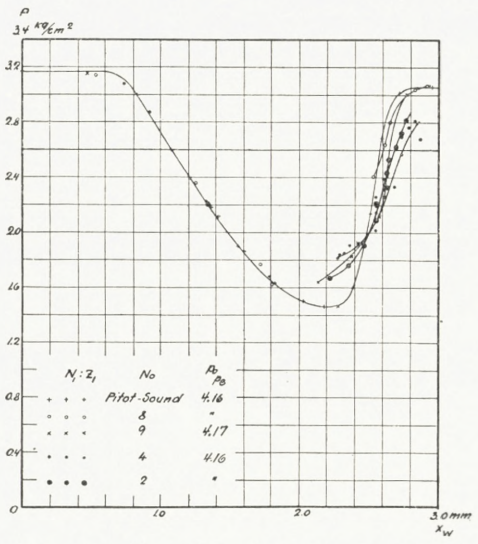

Fig. 41. Experimental Test of Conception with Regard to upper Reversion-Point.

Results of the comparison according to the method indicated are represented in figs. 40—41. In the figures the pitot-curve of the main-jet is reproduced. The points around or near the rising branch of the curves show the final pressures in the pulsator plotted against the final position of the wave in front of the pulsator-nozzle. The less the diameter of the cylindrical pulsator-nozzle, the closer to the pitot-curve are the points of observation as a rule.

With nozzles of about the same diameter as the jet, marked discrepancies occur. The latter are, however, much less pronounced with nozzles of types II and III than with such of type I.

In connection with the investigations of the upper point of reversal, determinations of the rear boundary of the interval of instability were made. It turned out that the said boundary was by far not as well-defined as the front of the interval. It seems, however, that the pulsations are apt to cease when the compression-wave which stands in front of the nozzle at the upper reversion-point has reached the boundary of the jet section.

In conclusion we desire to express our obligation to the Trustees of the Carlsberg Foundation for enabling us to carry out the present investigation by furnishing us with the necessary financial aid.

Physical Laboratory II of the Royal Technical College.

Copenhagen, Nov. 1928.

List of References.

1. Jul. Hartmann. Kgl. Danske Vidensk. Selsk. math.-fys. Medd. I. 13. (1919).
2. — Phys. Rev. 20. (1922). pg. 719.
3. — and Birgit Trolle. Kgl. Danske Vidensk. Selsk. math.-fys. Medd. VII. 6. (1926).
4. — — Journal of Scientific Instruments, Vol. IV. No. 4. Jan. 1927.
5. A. Stodola. Die Dampfturbinen. IV Auflage. Berlin 1910.
6. L. Prandtl. Handwörterbuch d. Naturwissenschaften. Bd. IV, pg. 544.
7. St. Venant & Wantzel. Journal de l'École Polytechnique, Vol. 16. 1839.
8. T. E. Stanton. Proc. of the Royal Soc. A. Vol. 111. 1926, p. 306.
9. L. Prandtl. Phys. Zeitschrift 1904. 599.
10. — Phys. Zeitschrift 1907. 23.
11. Th. Meyer. Inaugural Dissertation 1908.
12. E. Magin. — — 1908.
13. A. Steichen. — — 1909.
14. E. Mach u. P. Salcher. Wied Ann. 41. 1890, pg. 144.
15. R. Emden. Wied Ann. 69. 1899, pg. 426.
16. H. Parenty. Ann. chim. phys. 12. 1897. 289.
17. Riemann-Weber. Die partielle Differentialgleichungen. 5 Aufl. Bd. II, pg. 481. Braunschweig 1912.
18. Lord Rayleigh. Scientific Papers Vol. V, p. 573.
19. Handbuch d. Physik. B. VII, pg. 330. Berlin 1927.
20. Max Töpler. Ann. d. Physik 27. 1908. 1043.

Contents.

Færdig fra Trykkeriet den 7. Marts 1930.

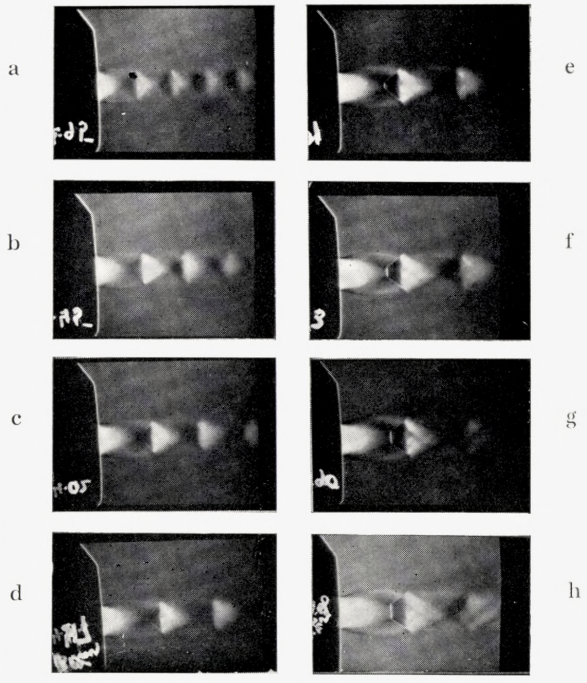

Fig. 4. The Pictures show the gradual Development of a perpendicular Compression-Wave and the breaking down of the regular Structure of the Jet. (See Tab. I).

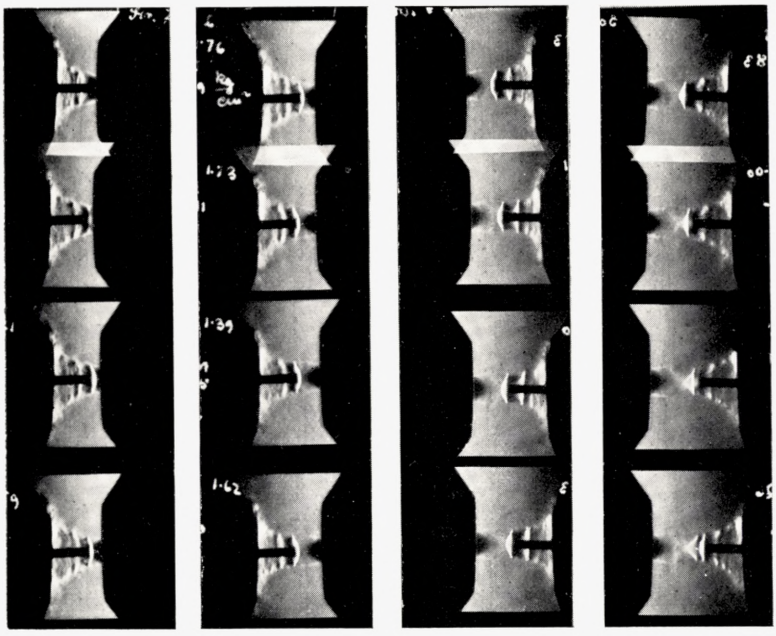

a b c d

Fig. 11. Photographs used in the Determination of a Pitot-Curve. Jet-Orifice *Z* I. Pressure in Container 4.26 kg/cm^2, x_p from 0.11 to 2.86 mm. Optical Screen perpendicular to Axis of Jet. Steel-Sound. (See Tab. II).

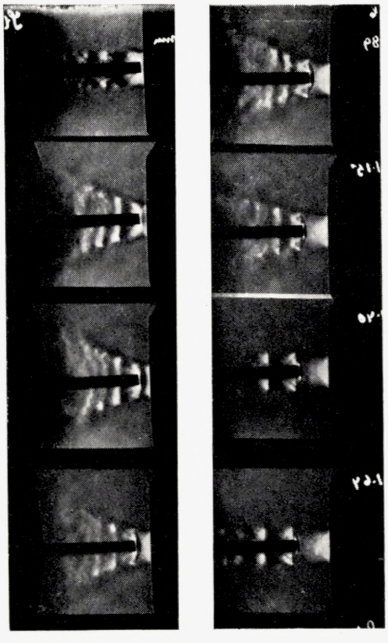

a b

Fig. 12. Photographs used in the Determination of a Pitot-Curve. Jet-Orifice *Z* I. Pressure in Container 4.28 kg/cm^2. x_p from 0.13 to 1.88 mm. Optical Screen perpendicular to Axis of Jet. Steel-Sound. (See Tab. II).

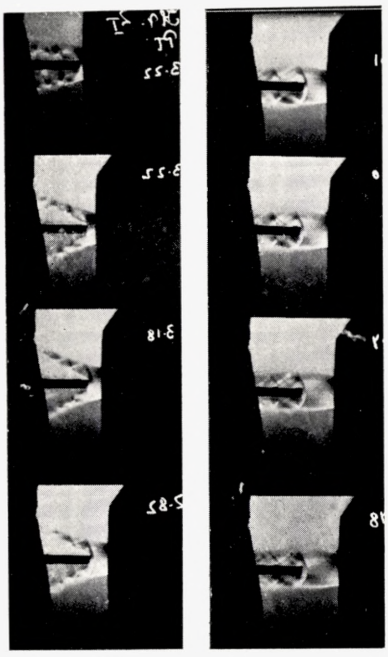

a b

Fig. 13. Photographs used in the Determination of a Pitot-Curve. Jet-Orifice *Z* I. Pressure in Container 4.21 kg/cm^2. x_p from 0.14 to 2.24 mm. Optical Screen parallel to Axis of Jet. Steel-Sound. (See Tab. II).

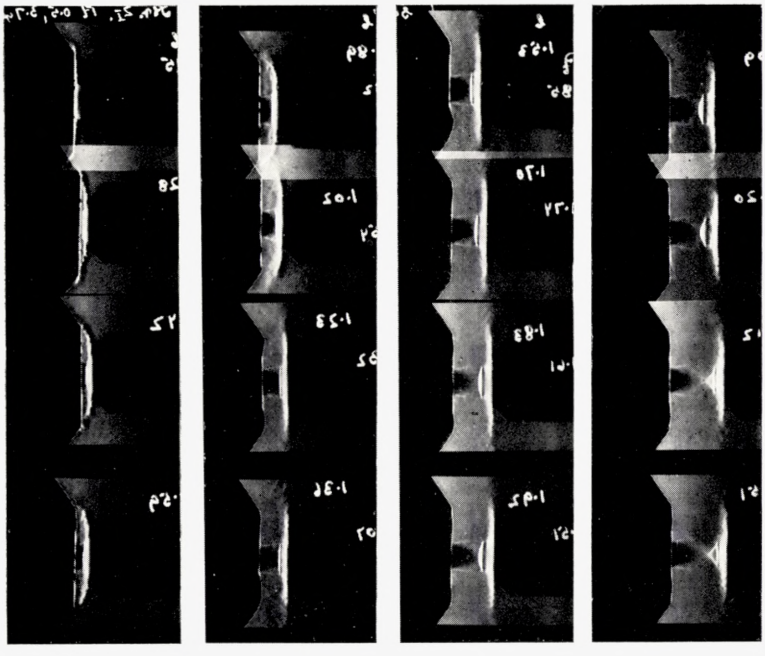

a b c d

Fig. 14. Determination of Part of a Pitot-Curve by Means of a Nozzle. Jet-Orifice *Z* I. Pressure in Container 3.23 kg/cm^2. Optical Screen perpendicular to Axis of Jet. (See Tab. II).

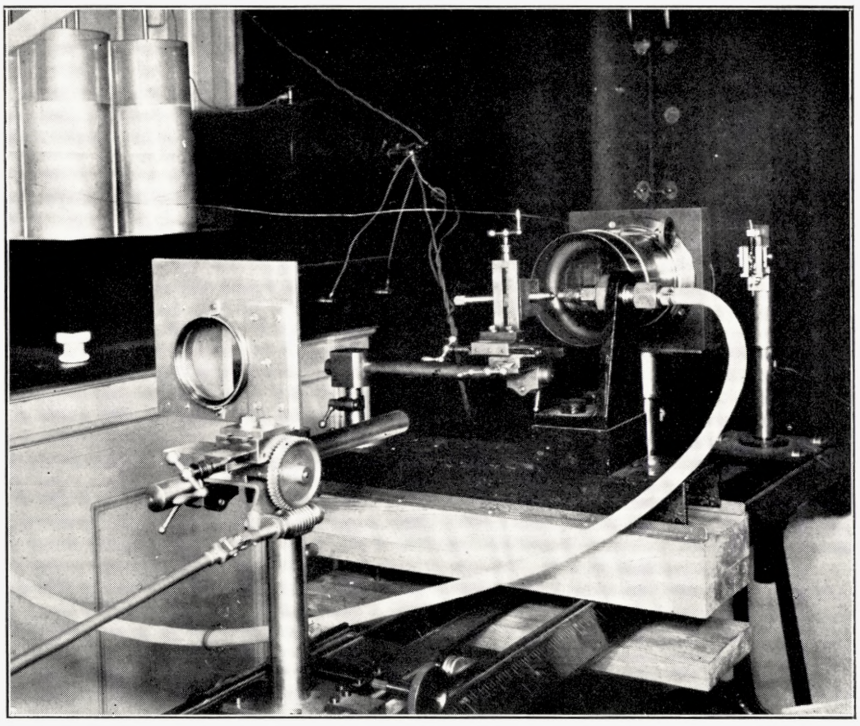

Fig. 21. Optical Arrangement.

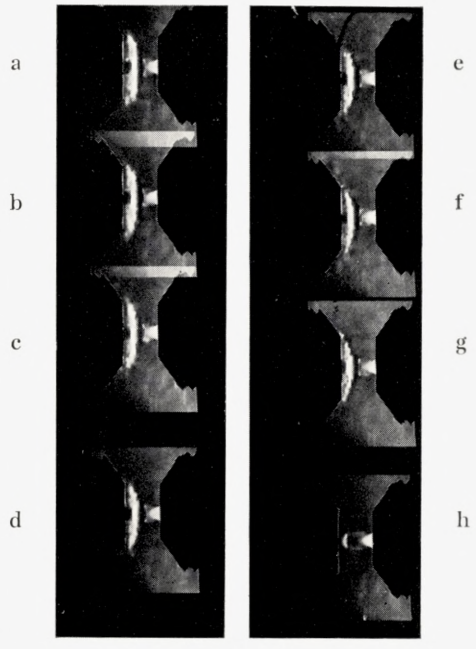

Fig. 28. The Pulsation-Process. Jet-Orifice Z_{I}. Pulsator Nozzle Z_{II}. $x_p = 4.48$ mm $p_0 = 4.26$ kg/cm^2. Consecutive Values of Pulsator-Pressure P: 2.92, 2.68, 2.48, 2.28, 2.08, 1.88, 1.68, 1.58 kg/cm^2 (Excess-Pressures).

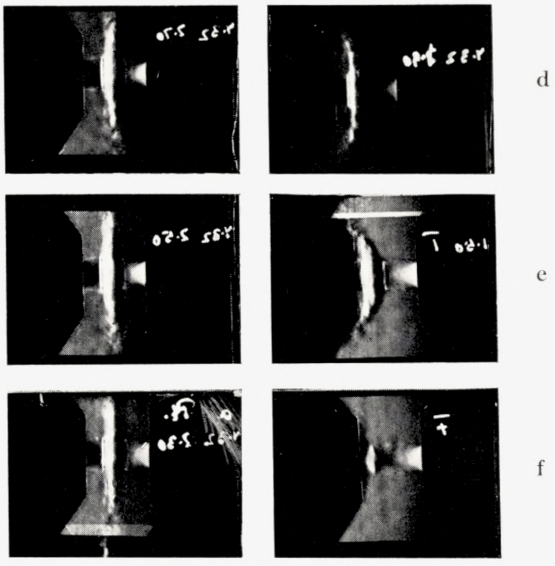

Fig. 29. The Pulsation-Process. Jet-Orifice Z_I. Pulsator-Nozzle No. 5, $x_p = 4.32$ mm, $p_0 = 4.28$ kg/cm^2. Consecutive Values of Pulsator-Pressure P: 2.70, 2.50, 2.30, 1,90, 1.50, 1.00 kg/cm^2 (Excess-Pressures).

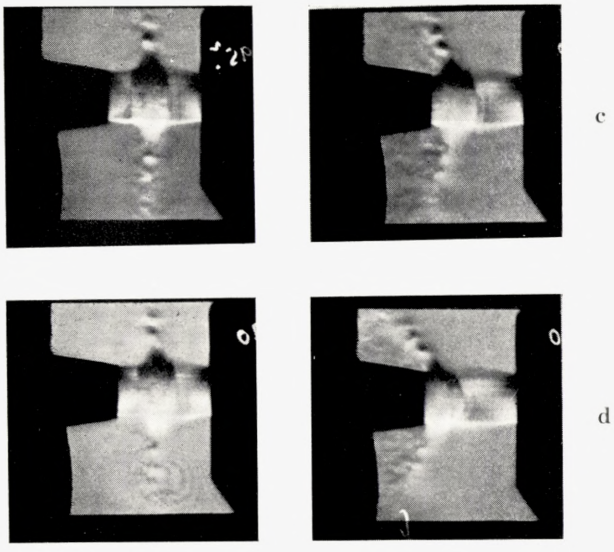

Fig. 30. The Pulsation-Process. Jet-Orifice Z_I. Pulsator-Nozzle No. 38, $x_p = 2.34$ mm, $p_0 = 4.26$ kg/cm^2. Consecutive Values of Pulsator-Pressure P: 2.95, 2.70, 1.70, 1.50 kg/cm^2 (Excess-Pressures).

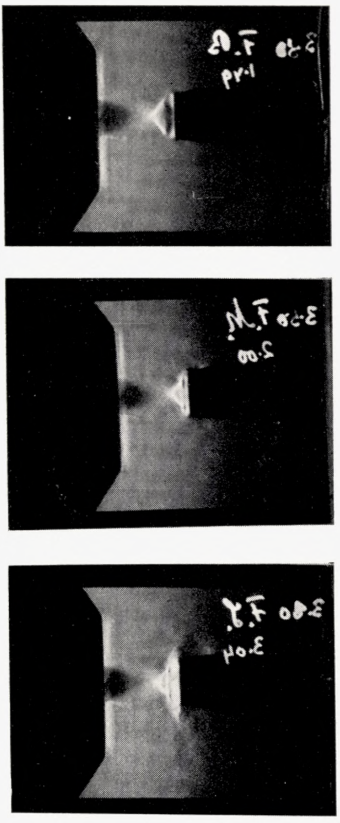

Fig. 38. Process of Filling. The Development and Motion of a Compression-Wave in Front of the Pulsator during the Filling. $N_1 = Z_1$. $N_2 =$ Nr. 38, $\frac{p_0}{p_e} = 4.15$.

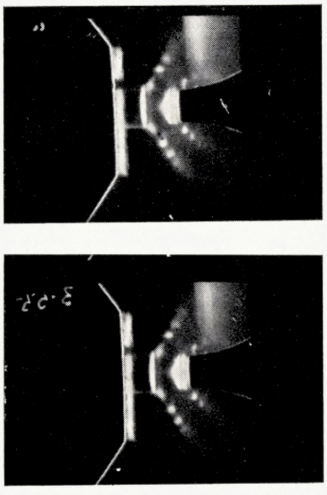

Fig. 39. Motion of the Compression-Wave near the End of the Process of Filling. $N_1 = Z_1$. $N_2 =$ Nr. 40. $\frac{p_0}{p_e} = 4.15$.